NATIONAL ADVISORY COMMITTEE FOR AERONAUTICS

TECHNICAL MEMORANDUM 1341

APPROXIMATE HYDRODYNAMIC DESIGN OF A FINITE SPAN HYDROFOIL

By A. N. Vladimirov

Translation

Priblizhennyi gidrodinamicheskii raschet podvodnogo kryla konechnogo razmakha. Central Aero-Hydrodynamical Institute, Report 311, 1937.

NACA

Washington

June 1955

NATIONAL ADVISORY COMMITTEE FOR AERONAUTICS

TECHNICAL MEMORANDUM 1341

APPROXIMATE HYDRODYNAMIC DESIGN OF A FINITE SPAN HYDROFOIL*

By A. N. Vladimirov

SUMMARY

Some problems concerning the motions of a hydrofoil are discussed. The results of theoretical investigations on motions of different bodies under a free surface of a heavy perfect fluid are revised, and for all cases diagrams of forces acting on moving bodies are given. The problem solved by Lamb for the motion of a circular cylinder and several problems solved during the last three years in the Central Aero-Hydrodynamical Institute (Moscow) are discussed. The latter are: the work by L. Sretensky on the motion of a vortex, the work by N. Kotchin on the motion of an arbitrary contour of streamline form (in the present article only a particular case of motion of a circular cylinder with a circulation around it is discussed), and the work by M. Keldysh and M. Lavrentiev on the motion of a plate and a circular aerofoil.

The analytical solution of the problem of motion of a plate is applied to an approximate hydrodynamic design of a hydrofoil, and on the basis of this solution diagrams are plotted allowing the determination of the lift and wave resistance of an infinite span hydrofoil during its motion in a fluid without friction.

Further, some considerations of the viscosity effect are given and a method of taking into account the finite span of the hydrofoil is suggested where an attempt is made at an approximate consideration of the effect of a free surface on the downwash behind a hydrofoil.

Further, some descriptions and experimental data for a hydrofoil tested in the CAHI tank are given and a comparison of theoretical with experimental data is made.

The described work forms a basis for an approximate hydrodynamic design of a finite span hydrofoil for small angles of incidence and for depths of immersion equaling and somewhat exceeding the chord length.

*Priblizhennyi gidrodinamicheskii raschet podvodnogo kryla konechnogo razmakha. Central Aero-Hydrodynamical Institute, Report 311, 1937.

INTRODUCTION

The hydrodynamic supporting forces act only on the lower surface of a planing boat. The supporting wings of airplanes are subject to the action of pressure forces on the lower surface and to suction forces on the upper surface. The motion of a planing profile inclined at a small angle of attack and the motion of the same body in infinite flow are considered here. The analogy established by Wagner (ref. 1) exists between the two flows considered.

From this analogy, with an accuracy up to second-order smallness, it follows that a planing foil during its motion is acted upon by a lift force A, a spray-forming resistance r, and the sum of all other resistances R, while a vane moving in an infinite flow is acted upon by a lift force 2A and the sum of all resistances 2R (all measured in kg); that is, it has no spray-forming resistance. The hydrodynamic efficiency of the planing foil k_1 is therefore equal to

$$k_1 = \frac{A}{R + r} \tag{a}$$

and the efficiency k_2 of the foil entirely submerged is equal to

$$k_2 = \frac{A}{R} \tag{b}$$

that is,

$$k_2 > k_1 \tag{c}$$

Investigations of the problem of increasing the speed of boats and lowering the power required by mounting hydrofoils on the bottom have been carried on abroad for some time. Investigations along this line are also being conducted in this country. The efficiency of hydrofoils decreases in the presence of the frontal resistance of the supports to which the vanes are attached. It is therefore desirable that during the motion of the boat the hydrofoils be located sufficiently near the free water surface. Because of the nearness of the free surface the hydrodynamic characteristics of the hydrofoil change; they do not follow the laws of motion of the same hydrofoil in an infinite fluid. The need therefore arises for an available method for the hydrodynamic computation of a hydrofoil on the basis of which the designer, by a computational procedure, could obtain the hydrodynamic polar curves of the foil selected for its motion at various depths of submersion. It is customary for the designer to have available the aerodynamic polar curves for the hydrofoil of interest.

If a body of streamlined shape, for example, a wing, moves in an infinite real fluid, the effect of the gravity force which shows up in

the Archimedean law of buoyancy can very simply be taken into account and only the effect of the forces of inertia and viscosity need be considered. There then holds true the well-known Reynolds law of similitude on the basis of which the forces exerted by the fluid on the wing or body are expressed by the formulas

$$\text{Lift force } A = C_y \rho S V^2$$

$$\text{Frontal resistance } R = C_x \rho S V^2$$

[NACA Translator's note: The more generally used coefficients today (1951) are twice the magnitude of the coefficients used in this report, since ρ is now replaced by $\rho/2$.]

where the nondimensional coefficients C_y and C_x are functions of the Reynolds number and the shape and position of the body. The scheme of an infinite flow of a weightless liquid is adopted in problems in which the flight dynamics of an airplane at large distance from the ground are considered. In studying the motion of a wing near the free surface of the water, it is necessary to take into account the action of the force of gravity on the fluid, because the wave disturbances of the free surface behind the wing alter in a fundamental way the hydrodynamics of the latter. It is known that in this case of motion, the forces exerted on the wing by the water are expressed by the formulas given. The nondimensional coefficients C_y and C_x, however, will in this case be functions not only of the Reynolds number but also of the Froude number. In the foreign literature on theoretical hydrodynamics there is very little information on the motions of bodies under the free surface of a heavy fluid. There is a particular lack of information on the problems of the motion of underwater wings (hydrofoils), and the papers available refer only to the circular cylinder. In regard to the history of this problem, a quotation is presented from the work of L. N. Sretensky (ref. 2):

"The problem here studied (the flow of a heavy fluid about an immersed circular cylinder)[1] is presented in literature. The problem was first posed by Keldysh in 1904 and was first solved by Lamb (ref. 3). The solution, given by Lamb, is approximate and consists of the addition to the potential of the infinite flow of a correction term, the object of which is to satisfy the condition at the surface. The introduction of this term, however, disturbs the conditions of flow about the cylinder.

"The next step in the solution of the problem was taken by Havelock (ref. 4). Making use of the methods of conformal mapping, Havelock extended the equation of Lamb by the addition of new terms with the purpose of setting up the conditions of flow about the cylinder. The solution of Havelock is also approximate, but the method indicated by him

[1]The remark in parentheses is ours.

can give an unlimited approximation to the complete solution of the problem if the extreme complexity of the formulas is disregarded. And further on, Lamb and Havelock, in presenting their approximate formulas, entirely omitted the velocity circulation about the cylinder."

There is still another series of papers by Havelock in which considered motions which give rise to the formation of waves are considered, but only the solution for the wave resistance is sought. Experimental work on hydrofoils has been carried out abroad, but the vanes were considered only in combination with various types of boats. No test data on isolated hydrofoils have been reported.

For the last three years work on the problem of the motion of bodies under the surface of a heavy fluid has made considerable progress at the CAHI. Approximate solutions have been given of the problems of the motion of a circular cylinder, a cylinder with velocity circulation about it, a thin plate, a circular disk, and, finally, an arbitrary profile of streamline shape. The workers at the CAHI test tank conducted tests in 1935 on the isolated underwater hydrofoil. The foil was towed at various angles of attack under various loads and measurements were made of the hydrodynamic forces (the lift and frontal drag) acting on the foil. The theoretical and experimental data available have been used in the present paper for investigating the essential character of the hydrodynamics of hydrofoils and for working out a method of the approximate hydrodynamic solution.

BRIEF REVIEW OF RESULTS OF THEORETICAL WORK

Only the theoretical investigations of interest for present purposes are considered. The feature common to all these investigations is the statement of the problem and the assumptions which make the solution approximate but permit reducing it to practical formulas. The authors consider the rectilinear and uniform motion of a body in a heavy, ideal, incompressible fluid at a certain depth from its free surface. Below the free surface the fluid is infinite in extent. The flow is assumed irrotational and most frequently plane-parallel. The boundary condition for the free surface is satisfied on the line of the undisturbed free surface. The velocities of the fluid particles on the free surface are so small that their squares may be neglected. Since the fluid is an ideal one and the flow possesses a potential, the frontal resistance encountered by the moving body is the wave resistance. If the fluid is infinite there is no wave resistance. In all the solutions given by the authors, the change in the lift force on the body with change of depth of submersion is set up and in each individual case the law of this change is given. Individual problems will now be considered.

Lamb considered the motion of a circular cylinder of radius r at the distance h from the free surface. The flow at a large distance from the cylinder has the velocity V; there is no circulation about the cylinder. The same case of motion was considered by M. V. Keldysh (ref. 5). The formulas obtained by Keldysh are the following:

$$A = -4\pi\rho a^2 \left[\left(\frac{1}{2h}\right)^3 + \left(\frac{1}{2h}\right)^2 \frac{g}{V^2} + \frac{1}{2h}\left(\frac{g}{V^2}\right)^2 - \left(\frac{g}{V^2}\right)^3 e^{-\frac{2gh}{V^2}} E_{i_1}\left(\frac{2gh}{V^2}\right) \right] \quad (1)$$

$$R = 4\pi^2\rho a^2 \left(\frac{g}{V^2}\right)^3 e^{-\frac{2gh}{V^2}} \quad (2)$$

where

A lift of cylinder, kg

R wave resistance, kg

a Vr^2

V velocity of flow at infinity, m/sec

r radius of cylinder, m

d diameter of cylinder, m

h distance from level of undisturbed surface, m

ρ mass density of fluid, kg sec^2/m^4

g acceleration of gravity, m/sec^2

π ratio of circumference of circle to diameter

E_{i_1} integral exponent of function (refs. 6 and 7)

The same notation will be used in what follows. The system of coordinates connected with the body is chosen in the usual manner; that is, the positive half-axis of ordinates y is directed upward and the positive half-axis of abscissas x is to the right. The flow past the cylinder is from left to right; the cylinder itself is stationary and its center has the coordinates $x = 0$, $y = -h$. The x-axis is placed along the free surface of the undisturbed fluid. As may be seen from formula (1), the lift force of the cylinder, for infinite submersion, is equal to

zero; that is, there is no velocity circulation about the cylinder. As the cylinder nears the free surface there first appears an insignificantly small positive lift force which then goes over into a negative one. The negative lift force increases monotonically in absolute value with decreasing depth. This is confirmed by the following considerations:

$$\frac{2gh}{V^2} = \tau \tag{d}$$

There follows from formula (1)

$$A = -4\pi\rho a^2 \frac{g^3}{V^6} f(\tau) \tag{e}$$

where

$$f(\tau) = \frac{1}{\tau} + \frac{1}{\tau^2} + \frac{1}{\tau^3} - e^{-\tau} E_{i_1}(\tau) \tag{f}$$

Since

$$E_{i_1}(\tau) = C + \ln \tau + \frac{\tau}{1} + \frac{1}{2}\frac{\tau^2}{2!} + \frac{1}{3} \cdot \frac{\tau^3}{3!} + \ldots +, \tag{g}$$

where C is the Euler constant, it is clear that for small τ

$$f(\tau) > 0 \tag{h}$$

To small values of τ there correspond small values of the depth h; therefore near the free surface the lift force of the cylinder is negative.

For very large τ there is the asymptotic equation

$$E_{i_1}(\tau) = \frac{e^{\tau}}{\tau}\left(1 + \frac{1}{\tau} + \frac{2!}{\tau^2} + \frac{3!}{\tau^3} + \ldots +\right) \tag{i}$$

Substituting this value of $E_{i_1}(\tau)$ in the expression for $f(\tau)$ gives

$$f(\tau) = -\frac{1}{\tau^3} - \frac{3!}{\tau^4} - \frac{4!}{\tau^5} - \ldots - \tag{j}$$

from which it is clear that for large τ

$$f(\tau) < 0 \tag{k}$$

Hence, for sufficiently large depth, the lift force of the cylinder is positive.

In order to study the behavior of the function $f(\tau)$,

$$f'(\tau) = e^{-\tau} E_{i_1}(\tau) - \frac{1}{\tau} - \frac{1}{\tau^2} - \frac{2}{\tau^3} - \frac{3}{\tau^4} \tag{l}$$

must be found and the function $g(\tau) = e^{\tau} f'(\tau)$

$$g(\tau) = E_{i_1}(\tau) - e^{\tau}\left(\frac{1}{\tau} + \frac{1}{\tau^2} + \frac{2}{\tau^3} + \frac{3}{\tau^4}\right) \tag{m}$$

must be investigated. The range of small τ is considered first. Since for small τ, $E_{i_1}(\tau)$ is of the order of $\ln(\tau)$, it is clear that

$$g(\tau) < 0 \tag{n}$$

and that

$$g'(\tau) = e^{\tau}\left(\frac{3}{\tau^4} + \frac{12}{\tau^5}\right) > 0 \tag{o}$$

Hence $g(\tau)$ increases monotonically in the range of small τ.

The range of very large τ is now considered. For this range,

$$g(\tau) = e^{\tau}\left(\frac{3}{\tau^4} + \frac{4!}{\tau^5} + \frac{5!}{\tau^6} + \ldots +\right) \tag{p}$$

that is,

$$g(\tau) > 0 \tag{q}$$

Hence $g(\tau)$, and therefore $f'(\tau)$, are negative in a certain interval $0 < \tau < \tau_0$ and positive for $\tau > \tau_0$; that is, $f(\tau)$ at first decreases and then increases.

In figure 1 is plotted a curve which shows that at a very large depth the lift force of the cylinder is positive and has a maximum at $\tau = 3.8$, that is, at the depth $h = 3.8\ V^2/2g$; at $\tau = 2.8$, that is, at the depth $h = 2.8\ V^2/2g$, the lift force of the cylinder becomes zero, and with further decrease of the depth it becomes negative.

Nondimensional magnitudes are used to construct the curves characterizing the hydrodynamic forces acting on the cylinder. The following concepts are introduced:

$$F = \frac{V}{\sqrt{2gd}} \tag{r}$$

the ratio

$$k = \frac{d}{h}$$

and the nondimensional coefficients of the lift and wave resistance of the cylinder

$$C_{yh} = \frac{A}{\rho d V^2} \qquad C_{rh} = \frac{R}{\rho d V^2} \tag{s}$$

From equations (1) and (2) are obtained

$$C_{yh} = -\frac{\pi}{32}\left[k^3 + k^2F^{-2} + kF^{-4} - F^{-6}e^{-\frac{F^{-2}}{k}}\,E_{i_1}\left(\frac{F^{-2}}{k}\right)\right] \tag{3}$$

$$C_{rh} = \frac{\pi^2}{32}F^{-6}\,e^{-\frac{F^{-2}}{k}} \tag{4}$$

The curves of the lift coefficients of the cylinder as a function of the ratio h/d for two values of the Froude number are constructed on the basis of formula (3) as shown in figure 2. The position of tangency of the cylinder to the undisturbed free surface corresponds to the ratio $h/d = 0.5$. As may be seen from the constructed curves the coefficients of the lift force directed downward attain their largest values near the free surface, exceeding the maximum values of the lift coefficients of airfoils. As has been stated previously, the curves must intersect the axis of abscissas. The points of intersection were not shown on the figure, since for $V/\sqrt{2gd} = 1.5$, $C_{yh} = 0$ only for $h/d = 6.2$; and for $V/\sqrt{2gd} = 5.0$, $C_{yh} = 0$ for $h/d = 70$.

The maxima of the positive lift coefficients are vanishingly small.

The curves of the coefficients of the wave resistance of the cylinder as a function of the Froude number for various ratios d/h are constructed on the basis of formula (4) in figure 3.

The position of contact of the cylinder relative to the undisturbed free surface corresponds to the ratio $d/h = 2$. Each curve of wave resistance coefficients has one maximum, the position of which is determined by the ratio

$$F = 1/\sqrt{3k}$$

The wave resistance itself for h = constant has a maximum with respect to the velocity, and the position of this maximum is given by

$$V = \sqrt{gh}$$

Far behind the cylinder the equation of the wave surface has the form

$$y = -\frac{4\pi g r^2}{V^2} e^{-\frac{gh}{V^2}} \sin \frac{gx}{V^2} \tag{5}$$

The maximum of the wave resistance corresponds to the maximum height of the wave which, as is easily seen, occurs at $V = \sqrt{gh}$. The velocity of propagation of the waves is equal to V and the length of the wave is

$$\lambda = 2\pi V^2/g$$

With this, the description of the results obtained for the motion of a circular cylinder without circulation is concluded.

The problem of the motion of a circular cylinder has also been solved by Sretensky. In it he introduced the circulation about the cylinder. The approximate solution obtained by the author justifies the conclusion that a cylinder with circulation produces the same flow disturbance as a vortex placed at the same depth. This result was obtained because for the degree of accuracy assumed by the author the terms which characterize the motion of the cylinder without circulation were rejected. Since the results of the work of N. E. Kotchin who retained the terms of Lamb in the problem solved by Sretensky are to be presented, the solution of Sretensky will be considered as the solution of the problem of the motion of a vortex near the free surface of a cylinder. The formulas obtained by Sretensky have the form

$$A = -\rho\Gamma V - \rho\Gamma^2 \left[\frac{1}{4\pi h} - \frac{g}{\pi V^2} e^{-\frac{2gh}{V^2}} E_{i_1}\left(\frac{2gh}{V^2}\right) \right] \tag{6}$$

$$R = \rho g \left(\frac{\Gamma}{V}\right)^2 e^{-\frac{2gh}{V^2}} \tag{7}$$

where Γ in square meters per second is the circulation about the vortex in its motion in an infinite flow.

The system of coordinates is chosen as in the preceding problem. The positive value of the circulation Γ corresponds to the counter

clockwise rotation (if the velocity of the approaching flow is directed from the left to the right of the observer). Hence, the sign of the Joukowsky lift force ($\rho\Gamma V$) is opposite to the sign of the circulation. For constructing the graphs characterizing the hydrodynamic forces acting on the vortex, we go over, as in the preceding problem, to the nondimensional magnitudes F and k. But for this purpose we first replaced, for convenience, the vortex by the supporting wing having the same circulation. On the basis of the Joukowsky theorem on the lift of a wing and the formula expressing the lift in terms of the nondimensional coefficient C_y, we then obtain

$$\Gamma = C_y bV = \pi\alpha bV \tag{t}$$

where b is the chord of the wing in meters and α is the angle of attack of the wing in radians.

After all transformations have been made, formulas (6) and (7) give

$$\frac{A + \rho\Gamma V}{(\alpha A_\infty)} = \left[\frac{1}{4}k - \frac{1}{2}F^{-2}\, e^{-\frac{F^{-2}}{k}} E_{i_1}\left(\frac{F^{-2}}{k}\right)\right] \tag{8}$$

$$\frac{C_{rh}}{C_y{}^2{}_\infty} = \frac{1}{2}F^{-2}\, e^{-\frac{F^{-2}}{k}} \tag{9}$$

where $F = V/\sqrt{2gb}$ and $k = b/h$.

The curves characterizing the change of the excess lift force of the wing, that is, the total lift after subtraction of the Joukowsky lift, are constructed as a function of the ratio h/b for two Froude numbers on the basis of formula (8) in figure 4. The constructed curves show that the free surface of the fluid gives rise to the appearance of an additional lift force (besides the Joukowsky force), the direction of which does not depend on the sign of the circulation (as is clearly seen from the structure of formula (6)). For small ratios h/b this additional lift force is directed downward; it then passes through zero and becomes positive. After forming a positive maximum it asymptotically approaches zero. On the basis of formula (9) there are constructed on figure 5 the curves characterizing the change in the coefficients of total resistance of the wing as a function of the Froude number for various values of the ratio b/h. Each curve has one maximum, the position of which is determined by the ratio $F = 1/\sqrt{k}$.

The wave resistance itself, as a function of the velocity, does not have a maximum and increases with increase in the velocity, asymptotically

approaching a constant value. This occurs because for a wing the circulation is proportional to the velocity only if the angle of attack and the chord are constant. If, however, the motion of a vortex is considered and the fact that the circulation about it Γ = constant is taken into account, the wave resistance, as a function of the velocity, will have a maximum, the position of which is determined by the relation

$$V = \sqrt{2gh}$$

Far behind the vortex, the equation of the wave surface is of the form

$$y = \frac{2\Gamma}{V} e^{-\frac{gh}{V^2}} \cdot \sin \frac{gx}{V^2} \tag{9a}$$

The maximum of the wave resistance corresponds to the maximum of the wave height, which, as is easily seen, occurs for $V = \sqrt{2gh}$. The velocity of propagation of the wave is equal to V and the wavelength $\lambda = 2\pi V^2/g$.

With this the description of the results obtained by L. N. Sretensky for the motion of a vortex is concluded.

N. E. Kotchin (ref. 8) gave general formulas for the hydrodynamic forces acting on profiles of arbitrary shape in a flow and selected the particular case of the motion of a cylinder of radius r with velocity circulation Γ about it. The formulas obtained by him for this particular case have the form

$$A = \rho\Gamma V - 4\pi a^2\rho \left[\left(\frac{1}{2h}\right)^3 + \left(\frac{1}{2h}\right)^2 \frac{g}{V^2} + \frac{1}{2h}\left(\frac{g}{V^2}\right)^2 - \left(\frac{g}{V^2}\right)^3 e^{-\frac{2gh}{V^2}} E_{i_1}\left(\frac{2gh}{V^2}\right)\right] -$$

$$\rho\Gamma^2 \left[\frac{1}{4\pi h} - \frac{g}{\pi V^2} e^{-\frac{2gh}{V^2}} E_{i_1}\left(\frac{2gh}{V^2}\right)\right] - \rho\Gamma V \left[\frac{1}{8}\left(\frac{2r}{h}\right)^2 + \frac{2gr^2}{V^2 h} - \right.$$

$$\left. \frac{4g^2r^2}{V^4} e^{-\frac{2gh}{V^2}} E_{i_1}\left(\frac{2gh}{V^2}\right)\right] \tag{10}$$

$$R = 4\pi^2 a^2 \rho \left(\frac{g}{V^2}\right)^3 e^{-\frac{2gh}{V^2}} + \rho g \left(\frac{\Gamma}{V}\right)^2 e^{-\frac{2gh}{V^2}} + \frac{4\pi\rho g^2 r^2 \Gamma}{V^3} e^{-\frac{2gh}{V^2}} \qquad (11)$$

The system of coordinates is chosen as in the preceding problems, but the direction of motion is opposite to the others. The sign of the Joukowsky lift force therefore agrees with the sign of the circulation. If in formulas (10) and (11) Γ is set equal to 0, there remain only terms not depending on Γ, and the formulas agree with formulas (1) and (2) for the forces acting on the cylinder without circulation. If in formulas (10) and (11) r is set equal to 0, there remain the terms not depending on r and the formulas agree with formulas (6) and (7) for the forces acting on a vortex.

The hydrodynamic forces acting on a cylinder with circulation will be described in somewhat greater detail. Formula (10) for the lift force may be written in the following form:

$$A = \rho\Gamma V + A_r + A_\Gamma + A_{r\Gamma} \qquad (12)$$

where $\rho\Gamma V$ is the Joukowsky lift force, A_r is the lift force of a cylinder of radius r without circulation (the same as by formula (1)), and A_Γ is the lift force of a vortex (the same as by formula (6)), and

$$A_{r\Gamma} = -\rho\Gamma V \left[\frac{1}{8}\left(\frac{2r}{h}\right)^2 + \frac{2gr^2}{V^2 h} - \frac{4g^2 r^2}{V^4} e^{-\frac{2gh}{V^2}} E_{i_1}\left(\frac{2gh}{V^2}\right)\right] \qquad (u)$$

that is, the lift force depending simultaneously on the radius of the cylinder and on the circulation about it.

From the preceding, the variations of the forces A_r and A_Γ are known. For very large depths of submersion of the cylinder, the force $A_{r\Gamma}$ has the same direction as the Joukowsky lift force; while for small depths it has the opposite direction.

For an explanation of this, it is necessary to consider the sign of the brackets in the expression for $A_{r\Gamma}$.

Setting

$$\frac{2gh}{V^2} = \tau \qquad (v)$$

leads to an investigation of the function

$$f(\tau) = \frac{1}{2\tau^2} + \frac{1}{\tau} - e^{-\tau} E_{i_1}(\tau) \qquad (w)$$

It is evident that, for small τ,

$$f(\tau) > 0 \tag{x}$$

since $E_{i_1}(\tau)$ is of the order of $\ln(\tau)$.

For large τ, the asymptotic formula

$$E_{i_1}(\tau) = \frac{e^{\tau}}{\tau}\left(1 + \frac{1}{\tau} + \frac{2!}{\tau^2} + \frac{3!}{\tau^3} + \ldots +\right) \tag{y}$$

is used to obtain

$$f(\tau) = -\frac{1}{2\tau^2} - \frac{2!}{\tau^3} - \frac{3!}{\tau^4} - \ldots \tag{z}$$

so that

$$f(\tau) < 0 \tag{a'}$$

Forming the derivative $f'(\tau)$ and investigating the function $g(\tau) = e^{\tau}f'(\tau)$ show that $f'(\tau) < 0$ in a certain interval $0 < \tau < \tau_0$ and $f'(\tau) > 0$ for $\tau > \tau_0$. Hence $f(\tau)$ at first decreases and then increases, having a negative minimum.

Formula (11) for the wave resistance may be written in the form

$$R = R_r + R_\Gamma + R_{r\Gamma} \tag{13}$$

where

R_r wave resistance of cylinder of radius r without circulation (same as by formula (2))

R_Γ wave resistance of a vortex (same as by formula (7))

$$R_{r\Gamma} = \frac{4\pi\rho g^2 r^2 \Gamma}{V^3} e^{-\frac{2gh}{V^2}} \tag{b'}$$

and the wave resistance depends simultaneously on the radius of the cylinder and on the circulation about it. For negative circulation the last part of the wave resistance $R_{r\Gamma}$ is also negative, and therefore the wave resistance of a cylinder with positive circulation is greater than the wave resistance of a cylinder with negative circulation. From formula (11) it also follows that under certain conditions of motion of the cylinder at a finite depth its wave resistance may be equal to zero. This

will evidently occur when the wave behind the cylinder will have a height equal to zero. Since the problem is solved on the basis of the linear theory of waves, the equation of the waves behind a cylinder with circulation can be obtained by taking the sum of the amplitudes of the waves behind a cylinder without circulation and behind a vortex. The right sides of equations (5) and (9a) are combined to obtain the equation of the waves behind a cylinder with circulation:

$$\nu = -\frac{2}{V} e^{-\frac{gh}{V^2}} \left(\Gamma + \frac{2\pi g r^2}{V}\right) \sin \frac{gx}{V^2} \tag{14}$$

The condition of motion for which the wave resistance of a cylinder with circulation is equal to zero is obtained by assuming the amplitude $y = 0$.

$$\Gamma = -\frac{2\pi g r^2}{V}$$

The same relation could have been obtained directly if the right side of expression (11) were set equal to zero. It is necessary to remark, however, that this condition does not give anything of practical value because it entirely fails to correspond to the real conditions of motion, at least in that the circulation Γ, and therefore the lift force, is negative.

In figure 6 the curves of the lift force and wave resistance of a cylinder of radius 0.1 meter with circulation $\Gamma = 0.25$ square meter per second are constructed as a function of the submersion h for constant velocity of motion $V = 6$ meters per second. The forces A and R are represented by their component parts. In figure 7 analogous curves are constructed for the same cylinder but with negative circulation, $\Gamma = -0.25$ square meter per second. The forces A_r, A_Γ, and $A_{r\Gamma}$ on these curves do not become zero because the zero points lie at a depth greater than 1 meter. The curves are given as an illustration of what has been said concerning the forces acting on a cylinder with circulation. With this, the description of the results obtained by N. E. Kotchin for the motion of a cylinder with circulation is complete.

The formulas for the hydrodynamic forces acting on a cylinder with circulation may be used to find the forces acting on a foil of chord b at angle of attack α moving with velocity V at depth h. For this purpose, the wing is replaced by a cylinder of diameter equal to the chord of the foil multiplied by α. The motion of the foil is considered under such small angles of attack that in the formulas for the forces it is possible to neglect the terms containing α of degree higher than the second. Substituting in formulas (10) and (11) the values $d = \alpha b$ and $\Gamma = \pi\alpha b V$ gives the formulas for the lift and wave resistance of a foil:

$$A = \pi\alpha\rho bV^2 \left\{1 - \alpha\left[\frac{b}{4h} - \frac{bg}{V^2} e^{-\frac{2gh}{V^2}} E_{i_1}\left(\frac{2gh}{V^2}\right)\right]\right\} \tag{15}$$

$$R = \pi^2\alpha^2\rho g b^2 e^{-\frac{2gh}{V^2}} \tag{16}$$

In these formulas only the terms depending on the circulation about the foil were retained, that is, the possiblity of neglecting the terms with degree of α higher than the second justifies replacing the foil by a vortex. If the motion of the foil is considered at somewhat greater angles of attack, when in the formulas for the forces it is possible to neglect only the terms containing α of degree higher than the third, then formulas (10) and (11) after substitution of $d = \alpha b$ and $\Gamma = \pi\alpha bV$ give

$$A = \pi\alpha\rho bV^2 \left\{1 - \alpha\left[\frac{b}{4h} - \frac{bg}{V^2} e^{-\frac{2gh}{V^2}} E_{i_1}\left(\frac{2gh}{V^2}\right)\right] - \alpha^2\left[\frac{b^2}{8h^2} + \frac{b^2g^2}{2V^2h} - \frac{b^2g^2}{\pi V^4} e^{-\frac{2gh}{V^2}} E_{i_1}\left(\frac{2gh}{V^2}\right)\right]\right\} \tag{17}$$

$$R = \pi^2\alpha^2\rho g b^2 e^{-\frac{2gh}{V^2}} + \pi^2\alpha^3\rho g^2 b^3 \frac{1}{V^2} e^{-\frac{2gh}{V^2}} \tag{18}$$

In these formulas only the Lamb terms are rejected. The rejected terms will be retained when it is necessary to take into account the fourth power of α; that is, the motion of a wing having a large value of $b\alpha$ is considered.

The last paper to be presented is that of Keldysh and Lavrentiev (ref. 9) on the motion of a thin contour under the free surface of a heavy fluid. The circulation consists of a system of vortices replacing the contour. The distribution of the vortices is such that one of the critical points is located at the rear edge of the contour. The circulation is therefore determined, and the hydrodynamic forces acting on the contour in its motion in the flow are expressed in terms of the geometric parameters defining the dimensions and position of the foil, that is, in terms of its chord and the angle of attack. The formulas obtained by the authors for the lift force and the wave resistance of a plane foil have the form

$$A = \pi\alpha\rho bV^2 \left\{ 1 - \frac{\pi gb}{V^2} e^{-\frac{2gh}{V^2}} - \frac{b^2}{16h^2} - \frac{gb^2}{4V^2h} + \frac{\pi^2 g^2 b^2}{V^4} e^{-\frac{4gh}{V^2}} + \right.$$

$$\left. \frac{g^2 b^2}{2V^4} e^{-\frac{2gh}{V^2}} E_{i_1}\left(\frac{2gh}{V^2}\right) - \alpha \left[\frac{b}{2h} - \frac{2gb}{V^2} e^{-\frac{2gh}{V^2}} E_{i_1}\left(\frac{2gh}{V^2}\right) - \right. \right.$$

$$\left. \left. \frac{\pi gb^2}{4V^2h}\left(4 + \frac{2gh}{V^2}\right) e^{-\frac{2gh}{V^2}} + \frac{4\pi g^2 b^2}{V^4} e^{-\frac{4gh}{V^2}} E_{i_1}\left(\frac{2gh}{V^2}\right) \right] \right\} \qquad (19)$$

$$R = \pi^2\alpha^2\rho gb^2 e^{-\frac{2gh}{V^2}} \left\{ 1 - \frac{2\pi gb}{V^2} e^{-\frac{2gh}{V^2}} + \alpha \left[\frac{gb}{2V^2} - \frac{b}{2h} + \right. \right.$$

$$\left. \left. \frac{2gb}{V^2} e^{-\frac{2gh}{V^2}} E_{i_1}\left(\frac{2gh}{V^2}\right) \right] \right\} \qquad (20)$$

and the simplified formulas

$$A = \pi\alpha\rho bV^2 \left\{ 1 - \frac{\pi gb}{V^2} e^{-\frac{2gh}{V^2}} - \alpha \left[\frac{b}{2h} - \frac{2gb}{V^2} e^{-\frac{2gh}{V^2}} E_{i_1}\left(\frac{2gh}{V^2}\right) \right] \right\} \qquad (21)$$

$$R = \pi^2\alpha^2\rho gb^2 e^{-\frac{2gh}{V^2}} \qquad (22)$$

Formulas (19) and (20) entirely agree with the formulas obtained if the aforementioned general solution of N. E. Kotchin on the motion of a contour of arbitrary shape is applied to the case of the plane foil.

Expressions (19) and (20) for the forces acting on the foil are approximate since they were obtained on the basis of the linear theory of waves, but they are, of course, closer approximations than the formulas (15) to (18) which were obtained by replacing the foil by a circular cylinder with circulation. This is explained by the fact that a cylinder with circulation is a system of a double source and vortex concentrated at one point, and no account is taken of the extension of the foil in the direction of the chord.

The expression for the forces acting on the foil, replaced by a system of vortices, is used for the approximate hydrodynamic computation of an underwater foil having infinite span. The lift force will be computed by formula (19) and the wave resistance by the simplified formula (22) which was obtained by replacing the wing by a vortex. The computation of the wave resistance by the more accurate formula (20) is of practically no advantage in view of the smallness of the terms which render it different from formula (22). Before the computation itself is presented, the difference is discussed between formula (18) of the wave resistance of a foil derived by replacing the wing by a cylinder with circulation and formula (21), obtained from the condition of replacing the foil by a system of vortices. On the basis of formula (18), the expression for the coefficient of the wave resistance of a foil replaced by a cylinder with circulation is

$$C_{rh} = M_r\alpha^2 + N_r\alpha^3 \tag{23}$$

where

$$M_r = \frac{\pi^2}{2} F^{-2} e^{-\frac{F^{-2}}{k}} \tag{24}$$

$$N_r = \frac{\pi^2}{4} F^{-4} e^{-\frac{F^{-2}}{k}} \tag{25}$$

It is evident that, for all values of the Froude number and the ratio b/h,

$$M_r > 0 \quad \text{and} \quad N_r > 0$$

Hence, with the coefficient of the wave resistance considered as a function of the angle of attack,

$$C_{rh}(\alpha) > C_{rh}(-\alpha) \tag{c'}$$

that is, for a wing replaced by a cylinder with circulation, the wave resistance for a positive angle of attack is always greater than for a negative angle of attack. On the basis of formula (20), an expression for the coefficients of the wave resistance of a foil replaced by a system of vortices is

$$C_{rh} = M_r\alpha^2 + N_r\alpha^3 \tag{26}$$

where

$$M_r = \frac{\pi^2}{2} F^{-2} e^{-\frac{F^{-2}}{k}} \left(1 - \pi F^{-2} e^{-\frac{F^{-2}}{k}} \right) \tag{27}$$

$$N_r = \frac{\pi^2}{2} F^{-2} e^{-\frac{F^{-2}}{k}} \left[\frac{1}{4} F^{-2} - \frac{1}{2} k + F^{-2} e^{-\frac{F^{-2}}{k}} E_{i_1}\left(\frac{F^{-2}}{k}\right) \right] \tag{28}$$

If as before

$$\frac{2gh}{V^2} = \tau \tag{d'}$$

the sign of the brackets in the expression for N_r(28) always agrees with the sign of the expression

$$f(\tau) = \tau + 4\tau e^{-\tau} E_{i_1}(\tau) - 2 \tag{28a}$$

Therefore

$$C_{rh}(\alpha) > C_{rh}(-\alpha) \quad \text{if} \quad f(\tau) > 0 \tag{e'}$$

$$C_{rh}(\alpha) < C_{rh}(-\alpha) \quad \text{if} \quad f(\tau) < 0 \tag{f'}$$

Formula (28) is used as a basis for constructing the curve of $f(\tau)$ on figure 8. However, in both cases the effect of the terms N_r is very small.

Three series of hydrodynamic polars of a hydrovane are constructed on the basis of formulas (19) and (22) on figure 9 to indicate the general form of the hydrodynamic forces acting on the foil in its motion near the free surface of an ideal fluid. Each series corresponds to a definite constant Froude number. The different polars of a single series correspond to different values of the ratio b/h. The dotted curves pass through the points of the same angles of attack. For all Froude numbers an increase of the ratio b/h (which for constant b corresponds to a decrease in the depth of submersion) gives rise to a decrease in the absolute values of the lift coefficients and an increase in the wave resistance coefficients. The coefficient C_{rh} does not depend on the sign of the angle of attack since the additonal terms were neglected, while C_{yh} for a negative angle of attack is always greater in absolute value than it is for a positive angle. The effect of an increase in the Froude number is to decrease the coefficients of the wave resistance of the foil while increasing the coefficients of the lift force in absolute value. This completes the review of results of theoretical work on the motion of bodies under the free surface of a heavy fluid.

CONSTRUCTION OF COMPUTATIONAL GRAPHS FOR MOTION OF A FOIL IN A PLANE-PARALLEL FLOW OF AN IDEAL FLUID

Formulas (19) and (22) are applied to the determination of the lift force and wave resistance of hydrofoils. For this purpose the nondimensional lift coefficient C_{yh} and wave resistance C_{rh} are employed. From formulas (19) and (22),

$$C_{yh} = \pi\alpha(M - N\alpha) \tag{29}$$

$$C_{rh} = \pi^2\alpha^2 \frac{gb}{V^2} e^{-\frac{2gh}{V^2}} \tag{30}$$

where

$$M = 1 - \frac{\pi gb}{V^2} e^{-\frac{2gh}{V^2}} - \frac{b^2}{16h^2} - \frac{gb^2}{4V^2h} + \frac{\pi^2 g^2 b^2}{V^4} e^{-\frac{4gh}{V^2}} + \frac{g^2b^2}{2V^4} e^{-\frac{2gh}{V^2}} E_{i_1}\left(\frac{2gh}{V^2}\right) \tag{31}$$

$$N = \frac{b}{2h} - \frac{2gb}{V^2} e^{-\frac{2gh}{V^2}} E_{i_1}\left(\frac{2gh}{V^2}\right) - \frac{\pi gb^2}{4V^2h}\left(4 + \frac{2gh}{V^2}\right) e^{-\frac{2gh}{V^2}} + \frac{4\pi g^2b^2}{V^4} e^{-\frac{4gh}{V^2}} E_{i_1}\left(\frac{2gh}{V^2}\right) \tag{32}$$

The question arises as to whether formulas (29) and (30), derived for plates, may be applied to the arbitrary profiles of hydrofoils. It is evident that they may more reliably be used for the computation of thin symmetrical profiles. In general, in the computation of each profile having a cross section different from that of plates, it is necessary to remember the following: In expression (29) the factor $\pi\alpha$ is the coefficient of the lift force of any profile in its motion in an ideal fluid for $h = \infty$. Formula (29) may therefore be written in the form

$$C_{yh} = C_{y\infty}(M - N\alpha) \tag{33}$$

In the computation of definite profiles for $C_{y\infty}$ it is necessary to take not the magnitude $\pi\alpha$, but the wind tunnel results for this profile,

the lift coefficients having first been computed for infinite span. In this manner the shape of the profile will be approximately taken into account. The section devoted to the consideration of the effect of the viscosity of the fluid will discuss this further.

Formula (30) for the coefficient of wave resistance may be represented in the form:

$$C_{rh} = C_{y^2\infty} \frac{gb}{V^2} e^{-\frac{2gh}{V^2}} \tag{34}$$

The $C_{y^2\infty}$ does not represent the magnitude $\pi^2\alpha^2$, but the square of the actual resistance coefficient of the wing of infinite span. Graphs were constructed for the convenient and rapid application of formulas (33) and (34) to the hydrodynamic computation of the hydrofoils. The magnitudes M and N are plotted as functions of the Froude number on the basis of formulas (31) and (32) for various values of the ratio b/h (figs. 10 and 11) to aid in computing the lift coefficients. To compute the coefficients of the wave resistance, the curves $C_{rh}/C_{y^2\infty}$ were constructed on the basis of formula (34) also as a function of the Froude number for various ratios b/h (fig. 12). The variations of the magnitudes F and k in the constructed graphs were taken in ranges which permitted obtaining the lift force and the wave resistance of hydrofoils of infinite span for all cases of motion of practical interest. The graphs constructed on figures 10, 11, and 12 representing formulas (33) and (34) thus permit obtaining approximately the lift force and wave resistance of a foil of infinite span moving near the free surface of an ideal fluid provided the lift coefficient for the motion of the wing in an infinite flow is known (e.g., from wind tunnel test data).

Effect of Viscosity of Fluid

A method for taking into account the effect of the viscosity of the fluid is now considered. The lift force of a foil in its motion in a real fluid depends little on the viscosity of the fluid since the lift of the foil is entirely determined by the potential circulatory flow about it. The viscosity appears to be only one of the factors giving rise to the circulation (ref. 10). The lift of the foil may therefore be obtained by the classical methods of hydrodynamics without introducing any corrections for the viscosity. A confirmation of this statement may be found in the comparison of the theoretical and experimental results on the determination of the lift of the wing. Betz (ref. 11), for example, carried out a computation of the pressures on the surface of wings of the Joukowsky type on the basis of the potential flow of an ideal fluid about the wing. He also made a comparison between his obtained results and

experimental data for the same wings. Good agreement was obtained. The slight increase of the theoretical lift force above that actually obtained is explained as caused by a separation of the flow which occurs at the upper surface of the wing not far from its trailing edge and this somewhat lowers the total pressure on the wing. All that has been said relative to the small dependence of the magnitude of the lift force of the wing on the viscosity of the fluid refers to the motion in an infinite flow. In the motion of the wing near a free surface, however, the effect of the viscosity on the lift force may likewise be regarded as practically absent because the change in the lift of the wing in its motion at a finite depth is brought about by a different pressure distribution on the wing different from the distribution which occurs in the motion at infinite depth (and gives the Joukowsky theorem). The other pressure distribution is due to the fact that the wave disturbances of the fluid remain behind and is not connected with the viscosity. It is true that in a real fluid the wave disturbances are damped, but this damping may be neglected for the case of water.

In the preceding section it was stated that $C_{y\infty}$ does not represent the magnitude $\pi\alpha$ but rather the result of wind tunnel tests on the foil. With this understood, the change in the lift of the wing due to the effect of the viscosity in its motion in an infinite flow is taken into account. The fact that no added corrections are made for the effect of the viscosity on the lift of the wing means only that the effect of the free surface on the lift is not connected with the viscosity. Thus in computing the lift force of a hydrofoil moving in a real fluid it is permissible to use the formula obtained for an ideal fluid without introducing any corrections for the viscosity except interchanging $\pi\alpha$ with the magnitude $C_{y\infty}$ obtained experimentally.

Accounting for the viscosity of the fluid for a certain total frontal resistance of the hydrofoil must be considered. For the present, the well-known considerations for the case of motion of a wing in an infinite flow are adduced. If the fluid is an ideal one, the foil during its motion is not subject to any frontal resistance, since it is known that in a potential flow the pressure at the forward part of the wing is equal in magnitude to the pressure at the after part. By a potential flow is here meant a nonseparated, nonvortical flow about the foil. The viscosity of the fluid is primarily the cause of the appearance of frictional resistance which is represented by the sum of the horizontal components of the forces tangential to the surface of the foil. Moreover, the viscosity brings about a general change in the potential flow about the wing. To these changes must be ascribed the formation of the boundary layer and the appearance of circulatory motions. Because of these changes in the flow, there is a change in the initial pressure distribution over the wing such that a frontal pressure resistance appears. The pressure resistance, together with the frictional resistance, is termed the form resistance. For wings of finite span the form resistance is divided into

the profile and induced resistances. As has already been said at the beginning of this paper, in the motion of a wing in an infinite flow the fluid may be considered as weightless and the Reynolds law of motion will then be valid. For the total frontal resistance of the wing the Reynolds law of motion gives the formula

$$R = C_x \rho S V^2$$

where the resistance coefficient C_x is a function of the shape of the foil, its position in the flow, and the Reynolds number. The similitude law of Reynolds consists of the following: If two wings are geometrically similar and their similar elements are inclined by equal angles to the direction of motion, and if the Reynolds numbers are equal, then there is complete similarity of the motions. In this case the drag coefficients for the two wings are the same. The values of the resistance coefficients of the wing for the different angles of attack are obtained from model tests in the wind tunnel, the tests being conducted at some single value of the Reynolds number near full scale. This is sufficient for the reason that at large angles of attack the drag coefficient depends little on the Reynolds number, while at small angles of attack when the flow is potential and the resistance is practically only the frictional drag, a correction for the change in the Reynolds number may be made by the known formulas for the resistance of a flat plate. It is understood, of course, that test results are entirely applicable when the foil model is tested for different values of the Reynolds number.

The motion of a wing in a real fluid near its free surface is now considered. Total frontal resistance of the foil is represented as the sum of three resistances: frictional, pressure, and wave resistances, although, generally speaking, such decomposition must not be made. It would be more correct to combine the pressure and wave resistances into one since they are similar in character; that is, they are brought about by the forces normal to the surface of the foil. Such formal decomposition must be considered, however, because of the absence at the present time of a solution of the problem of the motion of a foil near a free surface of a heavy real fluid. The manner in which the form resistance, that is, the pressure and frictional resistance considered apart from the wave resistance, varies in the transition of the foil from an infinite flow to the region near a free surface must be studied. The distribution of the streamlines changes and the velocity of the flow about the foil will be different. These changes in the flow give rise to changes in the frictional and pressure resistances; that is, it is necessary to take into account the fact that the dependence of the form resistance coefficient on the Reynolds number will be different from the corresponding relation for the motion of the same foil in an infinite flow. In reference to the nonvalidity of the separation of the wave resistance from the pressure resistance, there is no experimental possibility of separating these two resistances from each other and thereby obtaining the dependence of the

form resistance coefficient on the Reynolds number. On the basis of all that has been said there remains only the possibility of assuming that the coefficient of form resistance is the same as in the motion of the foil at infinite depth as it is at finite depth (of course, for the same Reynolds numbers) and that its dependence on the Reynolds number is in both cases expressed by the same law.

It can be said that the wave resistance arises from only the force of gravity and vanishes with increasing depth although the fluid continues to remain viscous. In a viscous, incompressible, heavy but infinite fluid, waves behind the moving foil cannot arise because their formation necessitates two layers of fluid of different densities. The viscosity will not be considered as the damping factor of the wave motions, since the motion of the wing in water where such damping may be practically neglected is considred. In this manner the wave resistance of the foil is assumed to not depend on the viscosity; and for determining the magnitude of the wave resistance, use is made of the theoretical formula obtained for the motion in an ideal fluid. For determining the over-all frontal resistance of a hydrofoil of infinite span, it is necessary to add to the wave resistance the form resistance, which is obtained from aerodynamic wind tunnel tests on the wing, initially computed for infinite span. If the data are available, corrections are made on the form resistance thus obtained for different Reynolds numbers in tests on the foil in a tunnel in relation to its motion in water.

Effect of the Finite Span of Hydrofoil

The finiteness of the span in its motion in an infinite fluid is taken into account by applying the theory of bound and free vortices. This theory was developed by L. Prandtl. The basis for this theory is the theorem of Joukowsky on the lift force of a wing applied to a wing of finite span and the theorem of Helmholtz on vortices. The physical picture of the formation of vortices may be obtained from the following considerations: In the presence of a lift force on the wing and therefore of a circulatory flow about it, there is a difference between the pressures on the upper and lower surfaces of the wing. Hence, at the tips of the wing the fluid will move from one surface onto the other in the direction of lower pressure. This transition of the fluid, because of its steady character, gives rise to the formation of a system of free vortices. Since, according to the theorem of Helmholtz, the vortices consist of the same particles of the fluid, the wing in its motion leaves behind it free vortices having a length equal to the path traversed by the wing. By the theorem of Helmholtz, the vortices cannot break away within the fluid; hence in the motion of the wing in an infinite flow the vortices either travel on with their ends at infinity or adhere to each other behind the wing to form closed systems. In the presence of a free surface of the fluid, the vortices may support themselves on the free

surface. The system of free vortices leads to the motion of the surrounding fluid and gives rise to a deflection or downwash of the flow approaching the wing. The downwash decreases the actual angle of attack and deflects the lift force behind the perpendicular drawn to the true direction of the motion of the wing. The projection of the lift force thus deflected on the direction of motion is the induced resistance of the wing. It is identical with the energy required to maintain the motion of the vortices. For all practical cases of the motion of a wing, the free vortices may be taken as half-filaments, that is, may be assumed as infinitely long, notwithstanding the finite interval of time from the starting instant of the motion. Actually, the velocity W induced by a segment of length c of the free vortex at a point distant h from its forward end is expressed by the formula

$$W_c = \frac{\Gamma}{4\pi h} \cdot \frac{c}{\sqrt{c^2 + h^2}} \tag{35}$$

If $c = \infty$, that is, the vortex is a half-filament, then

$$W_\infty = \frac{\Gamma}{4\pi h} \tag{36}$$

Set $c = nh$ and obtain the ratio W_c/W_∞:

$$\frac{W_c}{W_\infty} = \frac{n}{\sqrt{1 + n^2}} \tag{g'}$$

If, for example, $n = 5$, that is, if the length of the vortex is five times as large as h, $W_c/W_\infty = 0.98$; that is, the velocity induced by a finite vortex of length $c = 5h$ is 98 percent of the velocity induced at the same point by a half-filament. If the free vortex is supported on the free surface, its final length may be assumed as equal to a half-filament, since the point of support of the vortex remains in its place while the wing moves; therefore the length of the vortex rapidly attains practically an infinitely large value. The quantitative results of the theory of induced resistance are based on the magnitude of the induced velocity due to a straight vortex half-filament at any point of the surrounding fluid. For an infinite flow this velocity is expressed by formula (36). For a free vortex shed from the foil in its motion near a free surface, formula (36) is no longer applicable because the usual circular distribution of the streamlines about the vortex will be distorted by the presence of the free surface, and the magnitude of the induced velocity at any point of the fluid will therefore be other than in an infinite flow. The effect of the finite span of a hydrofoil is now considered. For simplicity, the wing of finite span is replaced by a horseshoe vortex which will consist of the actual vortices satisfying the theorem of Helmholtz. The horseshoe vortex moves near the free surface of the fluid. The resistance of the

free vortex is determined by theoretical formula (34) and there remains only to take into account the change in the flow about the principal vortex produced by the presence of the two free-vortex filaments remaining behind the foil. By the theorem of Helmholtz the vortices consist of the same particles of fluid, so that the free vortices do not follow behind the foil; that is, they do not have the property of forward motion in the direction of motion of the foil. If the effect of the free surface on the velocity field about the free vortices behind the foil is accurately taken into account, the problem will be a three-dimensional one. Wave disturbances remain behind the foil, and, considering some cross section of the free vortices in a plane perpendicular to the direction of motion of the foil, the level of the liquid will fluctuate because of waves from the foil. This wave motion will be neglected, however, and in considering the section of the free vortices in the above-mentioned plane, it is assumed that the foil does not leave behind it any wave disturbances; the problem will thus be a two-dimensional one. Moreover, the vortices are assumed to be stationary relative to the disturbed free surface. Each vortex is, in fact, situated in the velocity field of the other vortex and therefore they both have a tendency to move in a direction opposite to the direction of the lift force. This motion will be neglected in the same way it was in considering the flow downwash in aerodynamics. The free vortex is then considered as rigidly attached at the depth h under the free surface of the fluid.

Depending on the strength of the vortex, there will exist two limiting boundary conditions for the free surface of the fluid. For small values of circulation, the first boundary condition, which consists of the requirement that vertical velocities of the particles of the fluid on its free surface be absent, is obtained. In this case the free surface may be replaced by a rigid wall and the effect of the free vortex, by the effect of a pair of vortices of equal strength situated symmetrically with respect to the rigid wall and rotating in opposite directions. For large values of circulation, the second boundary condition, which consists of the requirement that horizontal velocities on the free surface be absent, is obtained. In this case the effect of the free vortex may be replaced by the effect of a vortex pair of equal strength situated symmetrically relative to the undisturbed free surface but rotating in the same direction. For the practical cases of motion of hydrofoils, the first boundary condition is more nearly applicable; but we shall nevertheless present both variants for taking into account the finiteness of the span in correspondence with the two boundary conditions with a view toward evaluating these variants in considering experimental data. The direct computation of the velocity induced by the free vortex will be discussed next. The characteristic stream function for a vortex pair of opposite rotation located at the points

$$x = 0,\ y = -ih \quad \text{and} \quad x = 0,\ y = ih$$

where $x + iy = z$, has the form

$$W_1 = \frac{\Gamma}{2\pi i} \ln \frac{z + hi}{z - hi} \tag{37}$$

The characteristic stream function for a vortex pair of the same direction of rotation located at the same points is

$$W_2 = \frac{\Gamma}{2\pi i} \ln(z^2 + h^2) \tag{38}$$

Consider the point of the fluid lying at the distance h from the level of the undisturbed free surface with abscissa x and find the velocity induced by the half vortex at this point. For this purpose the well-known relation

$$-\frac{\partial W}{\partial z} = u - iv \tag{39}$$

is used, where u is the horizontal velocity of the particles of the fluid, and v is the vertical velocity of the particles.

Applying this preceding relation to formulas (37) and (38) gives the corresponding vertical velocities induced by the half vortices:

$$V_1 = \frac{\Gamma}{4\pi} \left(\frac{1}{x} - \frac{x}{x^2 + 4h^2} \right) \tag{40}$$

$$V_2 = \frac{\Gamma}{4\pi} \left(\frac{1}{x} + \frac{x}{x^2 + 4h^2} \right) \tag{41}$$

In the case of the infinite flow, that is, for $h = \infty$, the expression

$$V = \Gamma/4\pi x$$

would be obtained in place of expressions (40) and (41).

Consider the foil at depth h with two free vortices trailing from its edges. Let the span of the foil be equal to l. In order to avoid obtaining, in the further computation, an infinitely large mean induced velocity over the foil span, it is necessary to assume that the distance between the free vortices $l' > l$. On the basis of equations (40) and (41), the mean value of the induced velocity over the wing span is obtained:

$$V_m = \frac{\Gamma}{2\pi l} \left[\ln \frac{l_1 + l}{l_1 - l} \mp \frac{1}{2} \ln \frac{t^2 + l^2 + 2lt + 4h^2}{t^2 + 4h^2} \right] \tag{42}$$

where

$$t = \frac{l_1 - l}{2} \qquad (h')$$

The minus sign refers to the first variant and the plus sign, to the second variant for taking into account the effect of the finite span.

It is known from tests that for the majority of foils,

$$\ln \frac{l_1 + l}{l_1 - l} \cong 4 \qquad (i')$$

whence

$$t \cong 0.025l \qquad (j')$$

Moreover, in the numerator of the second term of expression (42) the magnitude t^2 may be neglected because of its smallness. Then

$$V_m = \frac{\Gamma}{2\pi l}\left[4 \mp \frac{1}{2} \ln \frac{l^2 + 2lt + 4h^2}{t^2 + 4h^2}\right] \qquad (43)$$

Replacing t by $0.025\ l$ in expression (43) and introducing the chord of the foil b, the ratio $k = b/h$, and the aspect ratio $\lambda = l/b$ give the final expression for the mean induced velocity over the foil span

$$V_m = \frac{2\Gamma}{\pi l}\left[1 \mp \frac{1}{8} \ln \frac{1.05\lambda^2k^2 + 4}{0.000625\lambda^2k^2 + 4}\right] \qquad (44)$$

For an infinite flow, the induced velocity is computed by the formula

$$V_m = 2\Gamma/\pi l$$

The downwash angle of the flow β_{ih} and the induced drag C_{ih} (coefficient of induced drag) can now be readily found according to the physical sense of the downwash angle and the coefficient of induced drag to be

$$\beta_{ih} = \frac{V_m}{V_\infty} \qquad C_{ih} = \beta_{ih}C_{yh} \qquad (k')$$

where V_∞ is the velocity of motion of the foil. Hence, on the basis of expression (44) for the mean induced velocity, the expressions for the downwash angle and induced drag of the foil moving at depth h from the free surface are found to be

$$\beta_{ih} = \frac{2C_{yh}}{\pi\lambda}\left[1 \mp \frac{1}{8}\ln\frac{1.05\lambda^2k^2 + 4}{0.000625\lambda^2k^2 + 4}\right] \tag{45}$$

$$C_{ih} = \frac{2C_{yh}^2}{\pi\lambda}\left[1 \mp \frac{1}{8}\ln\frac{1.05\lambda^2k^2 + 4}{0.000625\lambda^2k^2 + 4}\right] \tag{46}$$

As seen from formulas (45) and (46), the angle of downwash and the induced drag of an underwater foil are either smaller or greater than the values of these magnitudes in the motion of a foil in an infinite flow depending upon the vortex scheme applied - either a vortex pair of opposite direction of rotation or one of the same direction of rotation. On figure 13 have been constructed the curves $\beta_{ih}/\beta_{i\infty} = f(h/b)$ for $\lambda = 6$ for the two variants under consideration. The same curves represent, of course, also the relation

$$\frac{C_{ih}}{C_{i\infty}} = f\left(\frac{h}{b}\right) \tag{1'}$$

To reduce the computation of the angle of downwash and the induced drag of a hydrofoil according to formulas (45) and (46), these formulas are rewritten in the form

$$\beta_{ih} = \frac{2C_{yh}}{\pi\lambda}(1 \mp \xi) \tag{45a}$$

$$C_{ih} = \frac{2C^2_{yh}}{\pi\lambda}(1 \mp \xi) \tag{46a}$$

where

$$\xi = \frac{1}{8}\ln\frac{1.05\lambda^2k^2 + 4}{0.000625\lambda^2k^2 + 4} \tag{46b}$$

On figure 14 the magnitude ξ has been constructed as a function of the product $\lambda k = l/h$. The use of this curve in the computation is clear from formulas (45a) and (46a).

Next, the relative error incurred if the usual formulas are used for determining the downwash angle and the induced drag of a hydrovane, with no account taken of the effect of the free surface on the magnitude of the induced velocity, will be obtained. For this purpose the following table is used:

$\lambda = l/b$	b/h = 0.5		b/h = 1.0		b/h = 2.0	
	I Method	II	I	II	I	II
2	3	3	11	9	25	17
5	15	11	33	20	67	29
10	33	20	67	29	93	32
15	52	25	111	34	190	40

For the various aspect ratios of the wing λ and ratio of wing chord to depth, the relative error is computed in percent for the downwash angle and the induced drag of the hydrofoil, using in place of formulas (45) and (46) the aerodynamic formulas. As may be seen, the relative error may attain a large value at large values of b/h, that is, near the free surface. The relative error increases with increasing λ but the absolute values of the angle of downwash and the induced drag decrease, and therefore the absolute error decreases with increasing λ. In considering the problem of accounting for the finiteness of the span of the hydrofoil, the following should be added: The downwash angle and the induced drag of hydrofoils must, as a rule, be determined by formulas (45) and (46) because the aerodynamic formulas would give a considerable error even for submersions equal to twice the chord of the wing. Such depth of submersion is already equal to the maximum suitable for use. Before anything can be said in regard to the final choice of boundary condition on the free surface determining the direction of rotation of a fictitious vortex, the experimental results must be considered. A computational example of a hydrofoil will be given also.

TANK TEST ON A HYDROFOIL

In 1935 tests were conducted by A. N. Vladimirov and V. G. Frolov at the CAHI tank on a plane underwater foil. The object of the test was to obtain the hydrodynamic characteristics of the foil at various submersions with a view toward mounting this foil on a seaplane. A thin symmetrical NACA 0.0009 profile of rectangular plan form having a chord $b = 0.14$ meter, span $l = 0.84$ meter, and therefore aspect ratio $\lambda = 6$ was tested. The thickness of the foil was 9 percent of the chord. On figure 15 are given the coordinates of this profile taken from the mentioned report. On figure 16 are given the aerodynamic characteristics of the profile obtained in the high pressure wind tunnel for a value of Reynolds number of 3.2×10^6, whereby A and R are denoted, as everywhere below, $A = C_y \rho S V^2$ and $R = C_x \rho S V^2$. For the tests in the tank the foil of the given dimensions was constructed of kolchugaluminum (an aluminum alloy) and was supported by two steel brackets which at their bases were fitted into the body of the foil from above, being attached to them by countersunk rivets and having at the places of juncture with the surface of the foil a smooth form. The scheme of arrangement of the brackets on the foil is shown in figure 17. The test was conducted on a special apparatus

which permitted measuring the lift and the frontal resistance of the foil with the brackets. The moment due to the hydrodynamic forces was not measured. The test setup is given on figure 18. The upper hinge axis of the vertical frame of the apparatus had one degree of freedom, that is, it could be displaced over an arc of sufficiently large radius. The impossibility of the deflection of the vertical frame toward one side was secured by a special device. For this reason the foil, being itself at constant angle of attack, that is, immovably connected with the vertical frame, had two degrees of freedom. The angle of attack of the foil was determined with an accuracy up to ± 8 minutes. The required depth of submersion of the foil was first approximately determined at standstill and in motion was measured with an accuracy up to ± 1 millimeter. By the depth of submersion of the foil is meant the distance of the geometric center of the foil from the level of the undisturbed free surface. The total frontal resistance of the foil with the submerged part of the brackets was measured by a contact dynamometer of the Gebers system. To the drum of this dynamometer was attached the towing rope, care being taken that the rope was always horizontal during the motion. Since the vertical frame was subjected to pressure from the air stream, this part of the resistance was experimentally taken into account. The hydrodynamic lift force of the foil was measured by a spring dynamometer with an accuracy up to ± 1 kilogram. For this purpose one measurement was made at standstill, that is, the load on the foil (weight of the structure) was determined, and another measurement was made during motion. The difference between the values of these measurements gave the magnitude of the lift force of the foil. The box on the vertical frame shown in the sketch was intended for the loads in the case where the positive lift (force directed upward) exceeded the weight of the structure. The length of the towing rope was so regulated that the axis of the principal frame of the apparatus occupied a vertical position. In the test setup used there was only one position of the foil when its center of pressure was displaced away from the vertical. The lift force was then somewhat deflected and therefore gave an additional resistance, which was taken into account by a special correction. The frontal resistance of the hydrofoil without support brackets was determined as the difference between the measured resistance of the foil with the brackets and the resistance of the brackets. The resistance of the brackets was computed by the formula $R = C_x \rho S V^2$, and C_x was determined from the air polars since the brackets constituted aeronautical profiles. The area S of the brackets was a function of the depth of submersion of the foil. It was assumed that there was no interference effect between the foil and the brackets. Since a wave remained after each test, an interval was required between the tests during which the surface of the water regained its calm.

The basic tests were conducted at constant towing velocity $V = 6$ meters per second. The depth of submersion of the foil was varied over a range from zero to the chord of the foil, and angle of attack was varied from -18° to $+18^\circ$. For small submersions the tests were restricted

to small angles of attack in order to maintain as far as possible complete submersion of the foil. Since the actual towing velocity for each test differed from $V = 6$ meters per second with a deviation up to 0.2 meter per second in either direction, all values of the lift force and resistance of the foil obtained in the measurements were recomputed for $V = 6$ meters per second on the assumption that in the interval of deviation of the velocity the hydrodynamic forces acting on the foil were proportional to the square of the velocity. Positive angle of attack was assumed in the usual sense of this term. For example, at an angle of attack of $+12^\circ$ the lift of the foil is directed upward; at -12° it is directed downward. In addition to tests at constant velocity, curves were obtained for the lift and drag of the foil as functions of the velocity for two different submersions h_1 and h_2. The angle of attack was here taken as constant and equal to 4°, and the velocity was varied in the range from 2 to 12 meters per second in 2-meter-per-second increments. All tests were conducted for constant submersion of the foil, that is, for each run the amount by which the load exceeded the lift was determined and the raising or submersion of the foil during the motion occurred only within the limits of the compression or extension of the springs of the dynamometer measuring the lift. The results of the tests on the hydrofoil are presented in the figures. On figures 19 and 20 are constructed the curves of the lift force A (in kg) and frontal drag R (in kg) of the hydrofoil as a function of the depth of submersion h (in mm) for various angles of attack α for constant towing velocity $V = 6$ meters per second. On figure 21 are constructed the curves of hydrodynamic efficiency of the hydrofoil as a function of the depth of submersion for two angles of attack $\alpha = +4^\circ$ and $\alpha = -4^\circ$. In this case, too, the towing velocity was constant ($V = 6$ m/sec). On figures 22 and 23 are constructed the curves of the lift force A (in kg) and frontal resistance R (in kg) of the hydrofoil as a function of the towing velocity for two different submersions $h_1 = 41$ and $h_2 = 82$ millimeters. The angle of attack was here constant and equal to 4°. For the present, an analysis of the experimental data obtained is not of concern, and the characteristic features of the constructed curves will not be explained; the discussion will be restricted to the presentation of the data. A comparison will subsequently be presented of the theoretical and experimental data, and it will then be easier to note the laws which govern the hydrodynamics of a hydrofoil.

The data obtained from the tank tests on the hydrofoil were valuable in that they brought out with particular clearness the effect of the most important factor, namely, the depth of submersion. The fact that the test was made on a thin symmetrical profile was a favorable circumstance. As a result, the conditions of the test very closely approached those for which the problem was theoretically solved. These favorable conditions were obtained in other tests on hydrofoils. For example, in the tank at Dumbarton (ref. 13), tests were conducted on a series of profiles for the scale effect, a part of the profiles being tested in a vertical position

and a part in a horizontal. The chord of the profiles tested in the horizontal position was equal to 16 centimeters and the submersion was constant at 60 centimeters, almost four times as large as the chord. The tests on the profiles under the free surface of water were in general repeated several times for the purpose of investigating the performance of propellers. The free surface of the water was, however, a necessity only in that it was unavoidable, and attempts were made to go as far as possible below the surface. In the present tests, however, an attempt was made to approach nearer the surface, and for this reason the possibility existed of clarifying the effect of the free surface and of comparing the experimental results with the theoretical.

HYDRODYNAMIC COMPUTATION PROCEDURE FOR THE HYDROFOIL

The first step is to recompute the air polars of the hydrofoil profile from finite to infinite span. On figure 24 are shown the curves of the lift coefficient of the foil for $\lambda = 6$ and the recomputed values for $\lambda = \infty$. The foil of infinite span has no induced drag so that the profile drag of the foil for $\lambda = \infty$ is obtained from the total drag for $\lambda = 6$ with the induced drag subtracted. After proceeding to the motion of the foil in a plane-parallel flow, the foil is transferred from the air to the water for, at first, infinitely great depth. There is a change in Reynolds number which, in agreement with a preceding section, must be taken into account. The air polar was obtained for a value $Re = 3.2 \times 10^6$.

In the water there is first of all a change in the coefficient of kinematic viscosity ν. For a temperature of the tank $t = 18^\circ$ C, $\nu = 0.013$ (cm^2/sec). Since the foil chord $b = 14$ centimeters, the velocity $V = 600$ centimeters per second is the following value for the Reynolds number $Re = Vb/\nu = 0.6 \times 10^6$.

The lift force of the foil is assumed not to change with the change in Reynolds number, and only the profile drag and that part of the profile which constitutes the friction drag are recomputed. The formula of Prandtl for the frictional drag coefficient of plane surfaces is used for this purpose (ref. 14). This formula includes the range of motion for the Reynolds numbers under consideration. The formula of Prandtl is of the form

$$C_f = \frac{0.074}{\sqrt[5]{Re}} - \frac{1700}{Re} \tag{47}$$

Recomputing by this formula the frictional drag of the foil gives the curve of profile drag for water. In figure 25 are constructed the profile drag curves for water and for air as functions of the angle of attack.

It should be remarked that the efficiency of the profile according to wind tunnel test data at the Reynolds number $Re = 3.2 \times 10^6$ was equal to 23 at an angle of attack of 4°. The hydrodynamic efficiency of the same profile for the Reynolds number $Re = 0.6 \times 10^6$ was equal to 18.2 as a result of the increase in the profile drag.

It is interesting to note that if the coefficient of the frictional drag of the foil is determined in its motion in air by formula (47), that is, for the same Reynolds number for which the air polar was obtained, then

$$100\ C_f = 0.32$$

while the actual profile drag coefficient of the foil for zero angle of attack is equal to

$$100\ C_f = 0.40$$

as seen from figure 25.

The total drag of the foil in its motion in air at zero angle of attack consists therefore of 80 percent frictional drag and 20 percent pressure drag arising from the thickness of the foil. At the same time, the value $100\ C_f = 0.32$ indicates the good agreement of the value of C_f obtained by the formula of Prandtl with the actual values and justifies the application of the Prandtl formula.

Since curves for the different towing velocities are still required, the curve of the profile drag of the foil as a function of the velocity in water at angle of attack of 4° has been constructed on figure 26. After the first stage of the computation, the hydrodynamic forces acting on a foil of infinite span moving in an infinite fluid are known.

It is now necessary to consider the motion of the foil when near the surface of the water. For this motion waves are formed behind the foil, the lift force of the foil changes, and a wave drag appears. The lift coefficient of a foil moving at depth h is obtained by means of the formula

$$C_{yh} = C_{y\infty}(M - N\alpha) \tag{33}$$

and the graphs shown in figures 10 and 11. The value $C_{y\infty}$ entering the formula is taken from the curve for $\lambda = \infty$ shown in figure 24. The coefficient of wave resistance of the foil is obtained by means of the formula

$$C_{rh} = C_{y\infty}^2 \frac{gb}{V^2} e^{-\frac{2gh}{V^2}} \tag{34}$$

and the curves constructed in figure 12.

In the tank tests on the hydrofoil, the depth of submersion was varied starting from zero. For comparison, however, the theoretical curves were constructed for only the submersion starting from 50 millimeters, since for smaller submersions formulas (33) and (34) will not give a correct result because the term

$$(b/2h)^3$$

and terms of higher degree were neglected in these formulas. The formulas may therefore be used only for those values of $b/2h$ which satisfy at least the inequality

$$b/2h < 1$$

Since the chord of the foil was $b = 140$ millimeters, the limiting case obtained for which these formulas may still be considered as valid is for a value of the submersion depth of

$$h = 70 \text{ mm}$$

In the computations deviations are made from the value $h = 70$ millimeters by another 20 millimeters. A closer approach to the free surface does not give anything even formally, since for this value M and N approach infinitely large values. The hydrodynamic forces acting on a foil of infinite span moving near the free surface of the water are now known.

The finite span of the foil must be taken into account; the change of its lift force due to downwash and the value of the induced drag are determined. The correction for the finiteness of the span was made for two variants corresponding to the two boundary conditions at the free surface. For the first variant, in which the free surface is replaced by a rigid wall, the downwash angle β_{ih} is always less at finite depth than the downwash angle for infinitely large depth. In both cases, of course, the same lift force is considered. For the second variant, in which the effect of the free surface is replaced by the effect of a vortex pair rotating in the same direction, the downwash angle β_{ih} at finite depth is always greater than the corresponding angle at infinitely large depth, again for the same lift forces.

The downwash angle behind the foil is found from the formula

$$\beta_{ih} = \frac{2C_{yh}}{\pi\lambda}(1 \mp \xi) \tag{45a}$$

and the curve on figure 14, where the magnitude ξ entering formula (45a) has been constructed as a function of the product λk. For the foil tested in the tank $\lambda = 6$ and $k = b/h$ depend on those depths h for which computational data are to be obtained. For each depth of submersion h there is a different downwash angle. The difference between one variant and the other is the fact that for the same depth of submersion of the foil, different values of the downwash angle are obtained. Having, for a given depth h, the lift curve of a foil of infinite span as a function of the angle of attack and knowing for this depth the magnitude of the downwash angle it is easy to construct the curve of lift force against the angle of attack for a foil of finite span, making use for this purpose of the usual graphical methods applied in aerodynamics. The computation is therefore individual for each depth.

The formula

$$C_{ih} = \frac{2C_{yh}^2}{\pi\lambda}(1 \mp \xi) \tag{46a}$$

and the curve $\xi = f(\lambda k)$ constructed in figure 14 are used to determine the induced drag of the foil. The computation is again conducted for each depth and, since the magnitude ξ entering the formula for C_{ih} is known, no difficulties are encountered. It is here likewise necessary to make use of the graphical methods applied in aerodynamics. A comparison of the thoretical curves with the experimentally obtained data will now be made.

COMPARISON OF THEORETICAL AND EXPERIMENTAL RESULTS

The lift forces are considered first. On figure 27 are given the theoretical curves for the lift force coefficients of the foil as a function of the submersion h in millimeters, and the test points are shown in the same figure. All data were reduced to the velocity $V = 6$ meters per second. There may first of all be observed the qualitative agreement. The lift force of a hydrofoil at all angles of attack decreases in absolute value with decrease in depth of submersion. A somewhat different character is possessed by the curve for zero angle of attack where the reverse phenomenon is indicated. Theoretically, for negative angles of attack the lift force should be greater than for the positive in absolute value, but this was not confirmed experimentally. In general, it must be said that the quantitative agreement of the theoretical with the experimental results is better the smaller the angle of attack and the larger the depth of submersion. This is understandable since the theoretical solution based on the linearized wave theory gives a better approximation when the foil produces a small disturbance. Best agreement of the results is given by the first variant ($\beta_{ih} < \beta_{i\infty}$).

Two theoretical curves and one experimental curve for the constant depth of submersion $h = 82$ millimeters and constant angle of attack 4° are constructed on figure 28 for comparison; these curves show the effect of the velocity of motion of the foil on its lift coefficient. From theoretical considerations it follows that the lift coefficient of the foil should increase with increasing velocity. The experimental curve actually has this tendency; however, it is only weakly indicated. The quantitative agreement very clearly speaks in favor of the first variant $(\beta_{ih} < \beta_{i\infty})$.

The data on the total drag of the hydrofoil are now compared. The theoretical curves of the coefficients of total drag of the foil are constructed as a function of the submersion h for the constant velocity of motion $V = 6$ meters per second on figure 29, and on the same figure are shown the test points. First noted is a characteristic feature of the theoretical and experimental results, namely, the increase of the drag coefficient of the foil with increase in depth of submersion. The increase is ascribed to the increase in the induced drag of the foil corresponding to the increase of its lift force with increased submersion. It is seen that starting from a certain depth the increase in the drag is discontinued and a drop begins as a result of the decreasing wave resistance. That such is the case is clear from the mutual positions of the curves and asymptotes. The quantitative agreement for positive angles of attack is as before better the smaller the angle of attack and the greater the depth of submersion. In comparing the drag for negative angles of attack, the opposite result is obtained. From the theoretical curves, it follows that

$$C_{xh}(\alpha) < C_{xh}(-\alpha)$$

which is explained by the fact that theoretically the lift force is greater for negative than for positive angles of attack, a fact which gives rise to the corresponding inequality in the induced drags. Experiment shows, however, that

$$C_{xh}(\alpha) > C_{xh}(-\alpha)$$

In the given case the experimental data obtained are assumed to be correct and the following explanation is given:

First of all, it is assumed that in taking account of the finite span the free surface is replaced by a solid wall. As has previously been pointed out, the downwash angle then decreases with approach of the foil (and therefore also the free vortices) to the surface; and for $h \to 0$, β_{ih} also $\to 0$. It was remarked also that the free vortices must possess a motion directed opposite to the lift force. Hence, for negative angles of attack the free vortices moving upward may approach very

near the free surface of the water and the downwash angle, and therefore also the induced drag, will be very small. From this it follows that the total drag of the hydrofoil for negative angles of attack will always be less than for positive angles. There is, unfortunately, as yet, no mathematical theory of this problem, nor does the possibility exist, on the basis of the above supposition, of finding the relation between the magnitude of the downwash angle for negative angle of attack and the depth of submersion of the foil.

On figure 30 are constructed two theoretical curves, and the test points of the drag coefficients of the foil are plotted for a constant submersion of the foil $h = 82$ millimeters and constant angle of attack 4°. From these data it is possible to learn the effect of the velocity of motion of the foil on its total drag coefficient. The theoretical curves give a decrease in C_{xh} with increase in velocity and a sharp increase in C_{xh} at small velocities. This is explained by the fact that for small Froude numbers, the coefficients of wave drag sharply increase. This was not confirmed experimentally. In the range of velocities starting from $V = 6$ meters per second and higher, good quantitative agreement is observed between the experimental data and the theoretical curve for the first variant ($\beta_{ih} < \beta_{i\infty}$).

On figure 31 are given the theoretical curves of the hydrodynamic efficiency of the hydrofoil as a function of the depth h for $\alpha = 4^{\circ}$ and velocity $V = 6$ meters per second. The test points are indicated also. The position of the test points confirms the general character of the theoretical curves. The quantitative agreement is better for the curve of the first variant, as has already been observed for the curves used as a basis for obtaining the curves of hydrodynamic efficiency.

On figure 32 the two diagrams are constructed so as to illustrate clearly the relations and changes in the parts of the total drag of the hydrofoil with change in depth of submersion of the wing. The curves are theoretically constructed for angle of attack $\alpha = 4^{\circ}$ and velocity $V = 6$ meters per second.

CONCLUSIONS

The comparison here given between the experimental and theoretical results of an investigation of the hydrodynamic forces acting on a hydrofoil has shown that the theoretical solution based on the theory of small waves gives an essentially correct representation of the phenomena occurring in the actual motion. The agreement of the results is less favorable with increase in angle of attack (in absolute value) and decrease in depth of submersion.

An attempt has been made in this paper to take into account approximately the finite span of the hydrofoil. The proposed method of finding the angle of downwash behind the hydrofoil is given simultaneously in two variants. For the velocities of motion considered the more accurate variant is that in which the free surface of the fluid is replaced by a rigid wall.

The viscosity of the fluid is taken into account in the usual manner, which is also approximate.

On the basis of the results obtained, it may be said that a reliable hydrodynamic computation of a hydrofoil may be made for those conditions of motion for which the absolute value of angle of attack is small and the depth of submersion is not less than the chord of the hydrofoil.

REFERENCES

1. Wagner, Herbert: Planing of Watercraft. NACA TM 1139, 1948.

2. Sretensky, L. N.: Motion of a Cylinder under the Surface of a Heavy Fluid. NACA TM 1335, 1952.

3. Lamb, Horace: Hydrodynamics.

4. Havelock, T. H.: Some Cases of Wave Motion Due to a Submerged Obstacle. Proc. Roy. Soc. (London), ser. A, vol. 93, 1917, pp. 520-532.

5. Keldysh, M. V.: Remarks on Certain Motions of a Heavy Fluid. Tech. Notes CAHI No. 52, 1935.

6. Shpilrein, Y. N.: Tables of Special Functions, Pt. I. Moscow, 1933, p. 9.

7. Jahnke und Emde: Functionentafeln mit Formeln und Kurven.

8. Kotchin, N. E.: On the Motion of a Contour of Arbitrary Shape under the Surface of A Heavy Fluid. Paper presented at CAHI (Moscow) 8/XII, 1935.

9. Keldysh, M. V., and Lavrentiev, M. A.: On the Motion of a Wing under the Surface of a Heavy Fluid. Paper presented at CAHI (Moscow) Jan. 1935.

10. Prandtl, L., and Tietjens, O. G.: Applied Hydro- and Aeromechanics. McGraw-Hill Book Co., Inc., vol. 2, sec. 107, 1935.

11. Betz, A.: Untersuchung einer Joukowskychen Tragfläche. Z.F.M.T. vol. 6, 1915, p. 173.

12. Jacobs, Eastman N., Ward, Kenneth E., and Pinkerton, R. M.: The Characteristics of 78 Related Airfoil Sections from Tests in the Variable-Density Wind Tunnel. NACA Rep. 460, 1933.

13. Allan, E.: Scale Effect in Screw Propellers. Trans. Inst. of Naval Architects, V, LXXVI, L. 1934, pp. 110-135.

14. Prandtl, L., and Tietjens, O. G.: Applied Hydro- and Aeromechanics. McGraw-Hill Book Co., Inc., vol. 2, sec. 68, 1935.

Translated by S. Reiss
National Advisory Committee
for Aeronautics

TABLE I. - VALUES OF M AND N FOR FORMULA (33)

$k=\frac{b}{h}$	$F=\frac{V}{\sqrt{2gb}}$	M	N	$k=\frac{b}{h}$	$F=\frac{V}{\sqrt{2gb}}$	M	N
0.2	∞	0.998	0.100	1.2	∞	0.910	0.600
	10.0	0.982	0.118		10.0	0.892	0.622
	7.5	0.972	0.122		7.5	0.881	0.628
	5.0	0.948	0.113		5.0	0.846	0.618
	3.0	0.910	0.046		3.0	0.735	0.525
	2.0	0.897	−0.073		2.0	0.650	0.255
	1.75	0.909	−0.119		1.75	0.620	0.121
	1.50	0.933	−0.159		1.50	0.594	−0.037
0.4	∞	0.990	0.200	1.4	∞	0.878	0.700
	10.0	0.974	0.224		10.0	0.859	0.721
	7.5	0.963	0.229		7.5	0.848	0.726
	5.0	0.935	0.228		5.0	0.813	0.713
	3.0	0.865	0.166		3.0	0.697	0.600
	2.0	0.814	0.039		2.0	0.608	0.293
	1.75	0.806	−0.027		1.75	0.579	0.132
	1.50	0.808	−0.091		1.50	0.550	−0.069
0.6	∞	0.978	0.300	1.6	∞	0.840	0.800
	10.0	0.961	0.324		10.0	0.821	0.819
	7.5	0.948	0.331		7.5	0.810	0.824
	5.0	0.913	0.333		5.0	0.773	0.810
	3.0	0.834	0.282		3.0	0.653	0.676
	2.0	0.768	0.108		2.0	0.561	0.318
	1.75	0.748	0.025		1.75	0.522	0.135
	1.50	0.739	−0.108		1.50	0.495	−0.117
0.8	∞	0.960	0.400	1.8	∞	0.798	0.900
	10.0	0.943	0.425		10.0	0.778	0.917
	7.5	0.930	0.431		7.5	0.767	0.919
	5.0	0.900	0.430		5.0	0.730	0.897
	3.0	0.804	0.359		3.0	0.605	0.752
	2.0	0.730	0.171		2.0	0.509	0.341
	1.75	0.704	0.092		1.75	0.471	0.131
	1.50	0.684	0.003		1.50	0.439	−0.154
1.0	∞	0.938	0.500	2.0	∞	0.750	1.000
	10.0	0 920	0.524		10.0	0.730	1.015
	7.5	0.908	0.530		7.5	0.718	1.014
	5.0	0.875	0.527		5.0	0.681	0.990
	3.0	0.771	0.446		3.0	0.552	0.824
	2.0	0.691	0.216		2.0	0.451	0.368
	1.75	0.662	0.111		1.75	0.412	0.130
	1.50	0.631	−0.003		1.50	0.375	−0.206

TABLE II. - VALUES OF C_{rh}/C_y^2 FOR FORMULA (34)

$k=\frac{b}{h}$	$F=\frac{V}{\sqrt{2gb}}$	$\frac{C_{rh}}{C_{y^2\infty}}$	$k=\frac{b}{h}$	$F=\frac{V}{\sqrt{2gb}}$	$\frac{C_{rh}}{C_{y^2\infty}}$
0.2	7.50	0.080	0.6	1.75	0.935
	5.00	0.161		1.50	1.042
	4.00	0.226		1.29	1.840
	3.00	0.314	0.8	7.50	0.086
	2.50	0.354		5.00	0.188
	2.23	0.363		4.00	0.285
	2.00	0.354		3.00	0.476
	1.75	0.316		2.50	0.646
	1.50	0.236		2.00	0.900
	1.20	0.100		1.75	1.070
	0.80	0.003		1.50	1.253
0.4	7.50	0.084		1.12	1.450
	5.00	0.178		0.90	1.280
	4.00	0.264		0.70	0.805
	3.00	0.416		0.60	0.414
	2.50	0.530		0.50	0.110
	2.00	0.660	1.0	7.50	0.086
	1.75	0.712		5.00	0.189
	1.58	0.725		4.00	0.290
	1.50	0.720		3.00	0.490
	1.20	0.610		2.50	0.674
	1.00	0.390		2.00	0.960
	0.80	0.154		1.75	1.162
	0.60	0.010		1.50	1.403
0.6	7.50	0.085		1.00	1.815
	5.00	0.184		0.60	1.840
	4.00	0.277	1.2	7.50	0.860
	3.00	0.456		5.00	0.191
	2.50	0.606		4.00	0.292
	2.00	0.811		3.00	0.500

TABLE II. - Concluded. VALUES OF C_{rh}/C_y^2 FOR FORMULA (34)

$k=\frac{b}{h}$	$F=\frac{V}{\sqrt{2gb}}$	$\frac{C_{rh}}{C^2_{y\infty}}$	$k=\frac{b}{h}$	$F=\frac{V}{\sqrt{2gb}}$	$\frac{C_{rh}}{C^2_{y\infty}}$
1.2	2.50	0.691	1.8	7.50	0.087
	2.00	1.000		5.00	0.193
	1.75	1.228		4.00	0.298
	1.50	1.510		3.00	0.515
	0.91	2.170		2.50	0.723
1.4	7.50	0.087		2.00	1.072
	5.00	0.191		1.75	1.340
	4.00	0.294		1.50	1.710
	3.00	0.505		0.74	3.260
	2.50	0.705		0.50	2.170
	2.00	1.032	2.0	7.50	0.087
	1.75	1.275		5.00	0.193
	1.50	1.590		4.00	0.298
	1.00	2.430		3.00	0.517
	0.84	2.540		2.50	0.730
	0.70	2.320		2.00	1.090
	0.60	1.860		1.75	1.365
	0.50	1.190		1.50	1.750
	0.40	0.300		1.20	2.400
1.6	7.50	0.087		1.00	3.020
	5.00	0.193		0.80	3.560
	4.00	0.296		0.70	3.630
	3.00	0.510		0.60	3.440
	2.50	0.715		0.50	2.660
	2.00	1.057		0.45	1.950
	1.75	1.311		0.40	0.124
	1.50	1.660		0.30	0.020
	0.79	2.900			
	0.50	0.162			

TABLE III. - VALUES OF ξ FOR FORMULAS (45a) AND (46a)

$\lambda k=\frac{l}{h}$	ξ	$\lambda k=\frac{l}{h}$	ξ
0.5	0.007	10	0.413
1.0	0.029	20	0.575
2.0	0.090	25	0.620
5.0	0.252	30	0.670

TABLE IV. - HYDRODYNAMIC CHARACTERISTICS OF HYDROFOIL MEASURED IN TOWING TESTS

Point	V,m/sec	h,mm	a, deg	R, kg	a, kg	Values of R for V=6m/sec, kg	Values of A for V=6m/sec, kg
1	6.07	±2	0	1.74	—	1.70	—
2	6.05	±2	— 2	1.18	—	1.16	—
3	6.04	1	2	2.90	— 15	2.86	— 14.8
4	6.00	0	4	4.79	— 4	4.79	— 4
5	6.01	—5	8	9.60	24	9.60	24
6	6.05	11	— 2	2.38	— 40	2.33	— 39.6
7	6.05	11	0	1.52	— 19	1.49	— 18.6
8	6.06	9	2	1.62	2	1.58	1.95
9	6.06	8	4	2.19	24	2.14	23.4
10	6.05	5	8	8.23	17	8.10	16.7
11	6.05	7	8	8.67	59	8.46	58
12	6.04	5	8	10.56	16	10.4	15.7
13	6.08	17	4	2.39	31	2.26	29.4
14	6.06	19	2	1.62	7	1.58	6.8
15	6.10	22	0	1.33	— 11	1.28	— 10.6
16	6.05	22	— 2	1.87	— 31	1.83	— 30.4
17	6.05	42	— 2	1.76	— 23	1.73	— 22.5
18	6.06	41	0	1.44	— 3	1.41	— 2.86
19	6.06	38	2	1.81	20	1.77	19.5
20	6.06	36	4	2.82	39	2.76	38
21	6.05	18	8	6.79	10	6.64	9.7
22	6.03	80	0	1.48	2	1.46	1.97
23	6.04	75	4	3.68	50	3.62	49.2
24	6.01	67	8	9.16	92	9.16	91
25	5.95	58	12	27.11	121	27.5	123
26	5.94	58	16	41.28	121	42.0	121
27	5.94	51	17.5	44.85	116	45.6	118
28	5.93	59	14	37.33	131	38.2	134
29	6.01	85	— 4	2.60	— 41	2.49	— 43.8
30	6.01	87	— 8	6.62	— 89	6.62	— 88
31	5.94	82	—12	18.05	—137	18.4	—139
32	5.93	69	—16	38.61	—156	39.4	—159
33	5.94	68	—18	37.54	— 96	38	— 97
34	5.98	83	—16.5	49.18	—167	49.2	—168
35	6.22	83	—16.5	46.65	—161	44.2	—149.5

TABLE IV. - Concluded. HYDRODYNAMIC CHARACTERISTICS OF HYDROFOIL MEASURED IN TOWING TESTS

Point	V,m/sec	h, mm	a, deg	R,kg	a, kg	Values of R for V-6m/sec, kg	Values of A for V-6m/sec, kg
36	6.15	83	−16.5	46.55	−161	44.0	−153.4
37	5.93	120	0	1.52	0	1.55	0
38	5.95	115	4	3.73	56	3.78	56.8
39	5.98	97	8	10.33	108	10.40	109
40	6.00	99	12	29.38	146	29.38	146
41	5.95	91	16	44.48	136	45.2	138
42	5.93	91	16	44.38	136	45.2	138
43	5.96	90	17.5	48.17	124	48.8	126
44	6.02	94	14	38.75	145	38.5	144
45	6.04	125	− 4	2.70	− 58	2.66	− 57.2
46	5.98	127	− 8	7.18	− 110	7.2	−111
47	5.97	125	−12	21.00	−151	21.2	--153
48	6.00	119	--16	42.86	−171	42.86	−171
49	6.02	112	20	54.80	−151	54.4	−150
50	6.08	150	0	1.72	0	1.67	0
51	6.05	142	4	3.88	59	3.82	58.4
52	6.04	137	8	10.80	113	10.6	111
53	6.01	127	12	30.56	143	30.4	142
54	6.04	121	16	46.70	138	46	136
55	5.98	123	17.5	50.33	132	50.6	133
56	6.04	155	− 4	2.80	− 54	2.76	− 53.2
57	6.09	156	− 8	7.68	−122	7.45	−118
58	6.00	154	−12	23.50	−166	23.5	−166
59	6.00	151	−16	45.47	−174	45.47	−174
60	5.95	141	−18	51.85	−173	52.6	−175
61	1.98	43	4	0.28	4	—	—
62	4.05	39	4	1.25	17	—	—
63	6.08	43	4	2.90	45	—	—
64	8.05	41	4	4.83	80	—	—
65	10.10	44	4	7.18	124	—	—
66	12.12	35	4	9.80	165	—	—
67	2.04	85	4	0.38	6	—	—
68	4.12	82	4	1.60	26	—	—
69	6.15	81	4	3.37	60	—	—
70	8.06	82	4	5.77	102	—	—
71	10.20	85	4	8.41	155	—	—
72	12.10	77	4	13.89	240	—	—

TABLE V. - CHARACTER OF FLOW ABOUT HYDROFOIL IN TANK TESTS

Point	Condition of motion	Remarks
1	h=0, $\alpha=0^{\circ}$, V=6m/sec	Spray film from leading edge of foil in upward direction. Foil undergoes vertical vibration with amplitude of 2 millimeters.
2	h=0, $\alpha=-2^{\circ}$ V=6 m/sec	Spray film from leading edge inclined somewhat backward. Vertical vibration as under 1.
3	h=0, $\alpha=4^{\circ}$, V=6 m/sec	Spray film from leading edge inclined somewhat forward. Vibration of foil discontinued.
6	h=11 mm, $\alpha=-2^{\circ}$, V=6 m/sec	From the leading edge of the foil a film adhering to the upper surface is formed.
10	h=5 mm, $\alpha=8^{\circ}$, V=6 m/sec	From the trailing edge of the foil a film is formed having a horizontal direction. From the leading edge a film is formed making with the chord an angle of 45° and forming a water arch over the foil.
13	h=17 mm, $\alpha=4^{\circ}$, V=6 m/sec	The flow about the foil is smooth, a vertical film being formed at each bracket. This smooth character of the flow occurs in all cases where the angle of attack is not too large and the foil is submerged at a sufficient depth.
25	h=58 mm, $\alpha=12^{\circ}$, V=6 m/sec	Behind the foil there is a depression which, after 3 meters, ends in turbulence.
26	h=58 mm, $\alpha=16^{\circ}$, V=6 m/sec	Behind the foil there is a depression covered with jets running off the foil. At a distance of about 1 meter the jets are transparent and beyond that point have a foamy structure.
27	h=51 mm, $\alpha=17.5^{\circ}$, V=6 m/sec	From the middle of the foil over the entire span vortical filaments similar to systems of free vortices are formed. A group of such vortices does not adhere strongly to the foil and periodically breaks away, and in its place new vortices are formed.
33	h=68 mm, $\alpha=-18^{\circ}$ V=6 m/sec	From the lower surface of the foil (the low-pressure surface), a vortex film periodically breaks away as under 27. This phenomenon is the cause of the vertical vibration of the foil.

TABLE V. - Concluded. CHARACTER OF FLOW ABOUT HYDROFOIL IN TANK TESTS

Point	Condition of motion	Remarks
47	h=125 mm, $\alpha=-12^{\circ}$, V=6 m/sec	Flow about the foil is smooth. Immediately behind the foil a ridge is formed which at approximately $1\frac{1}{2}$ meters becomes a depression.
48	h=119 mm, $\alpha=-16^{\circ}$, V=6 m/sec	The same as under 47.
49	h=112 mm, $\alpha=-20^{\circ}$, V=6 m/sec	Immediately behind the foil a ridge is formed going over farther into a depression. Behind the foil vortical filaments were observed which, however, started not from the foil itself but approximately 1 meter behind the foil.
52	h=137 mm, $\alpha=8^{\circ}$, V=6 m/sec	The flow about the foil is smooth. Immediately behind the foil is a shallow depression ending in surf.
61 to 72	$\alpha=4^{\circ}$	The flow about the foil is very smooth and the course is constant. A small vertical film is formed at each bracket.

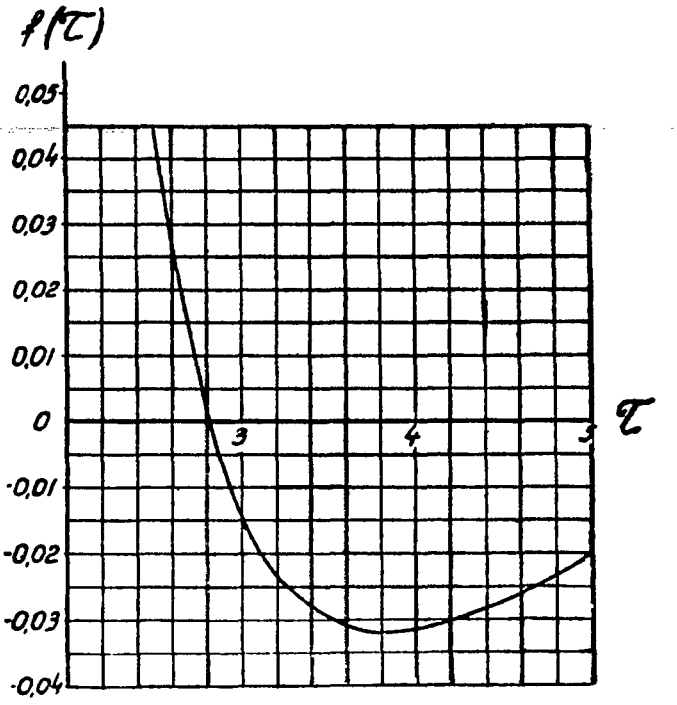

Figure 1. - Effect of $\tau = 2gh/V^2$ on lift force of a cylinder without circulation.

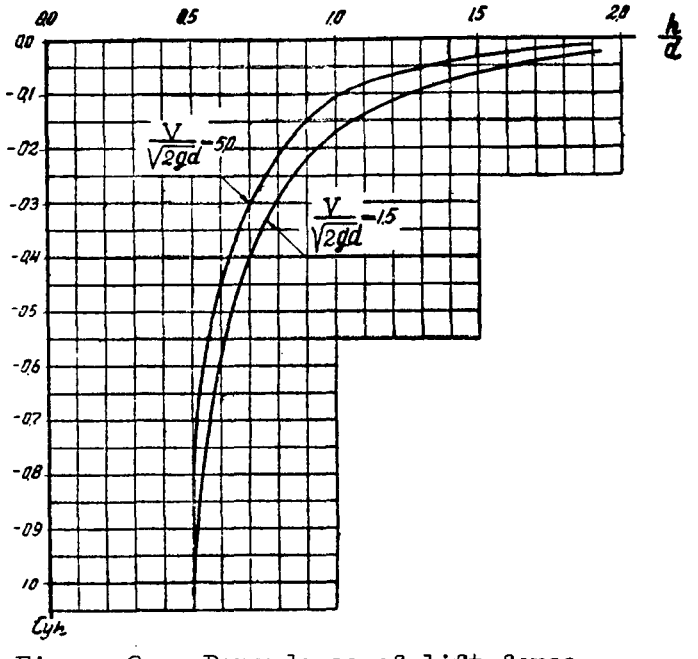

Figure 2. - Dependence of lift force coefficient of a cylinder without circulation on h/d and $V/\sqrt{2gd}$.

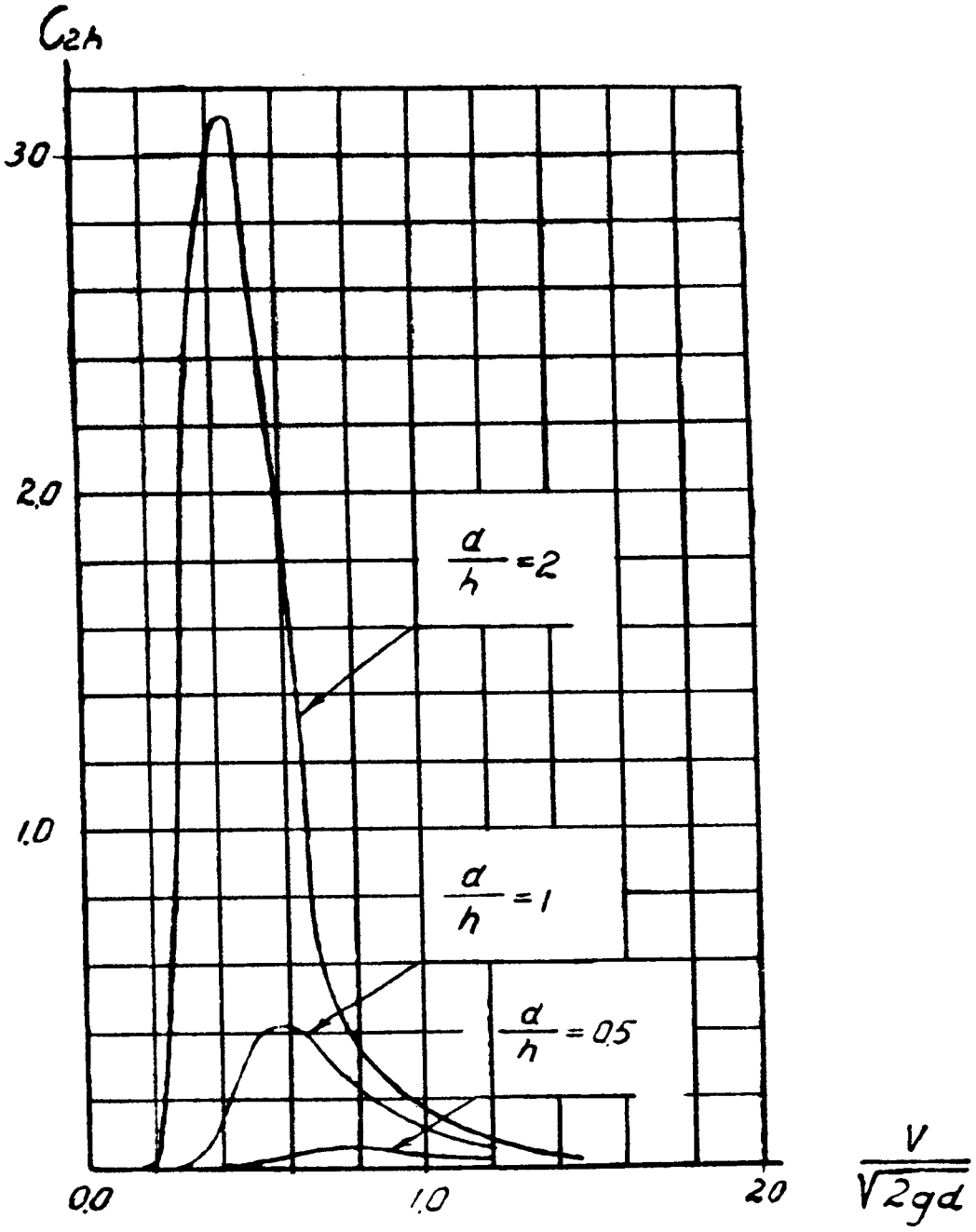

Figure 3. - Dependence of wave drag coefficient of a cylinder without circulation on d/h and $V/\sqrt{2gd}$.

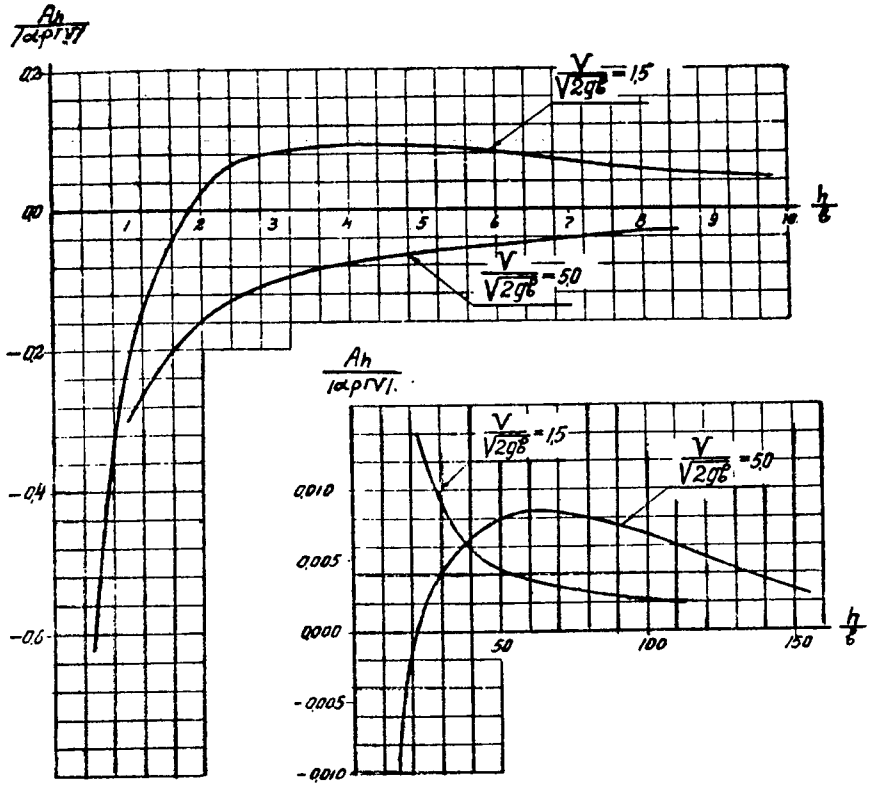

Figure 4. - Dependence of lift of a foil replaced by a vortex on h/b and $V/\sqrt{2gb}$.

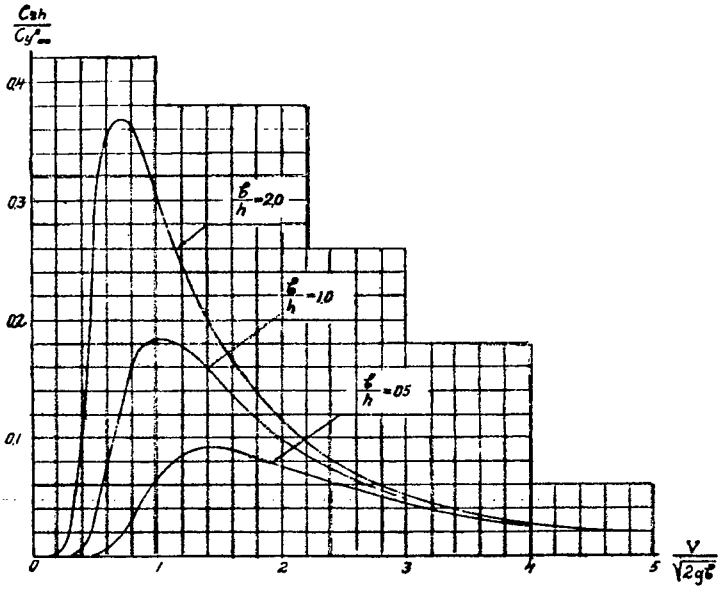

Figure 5. - Dependence of wave drag coefficient of a foil replaced by a vortex on b/h and $V/\sqrt{2gb}$.

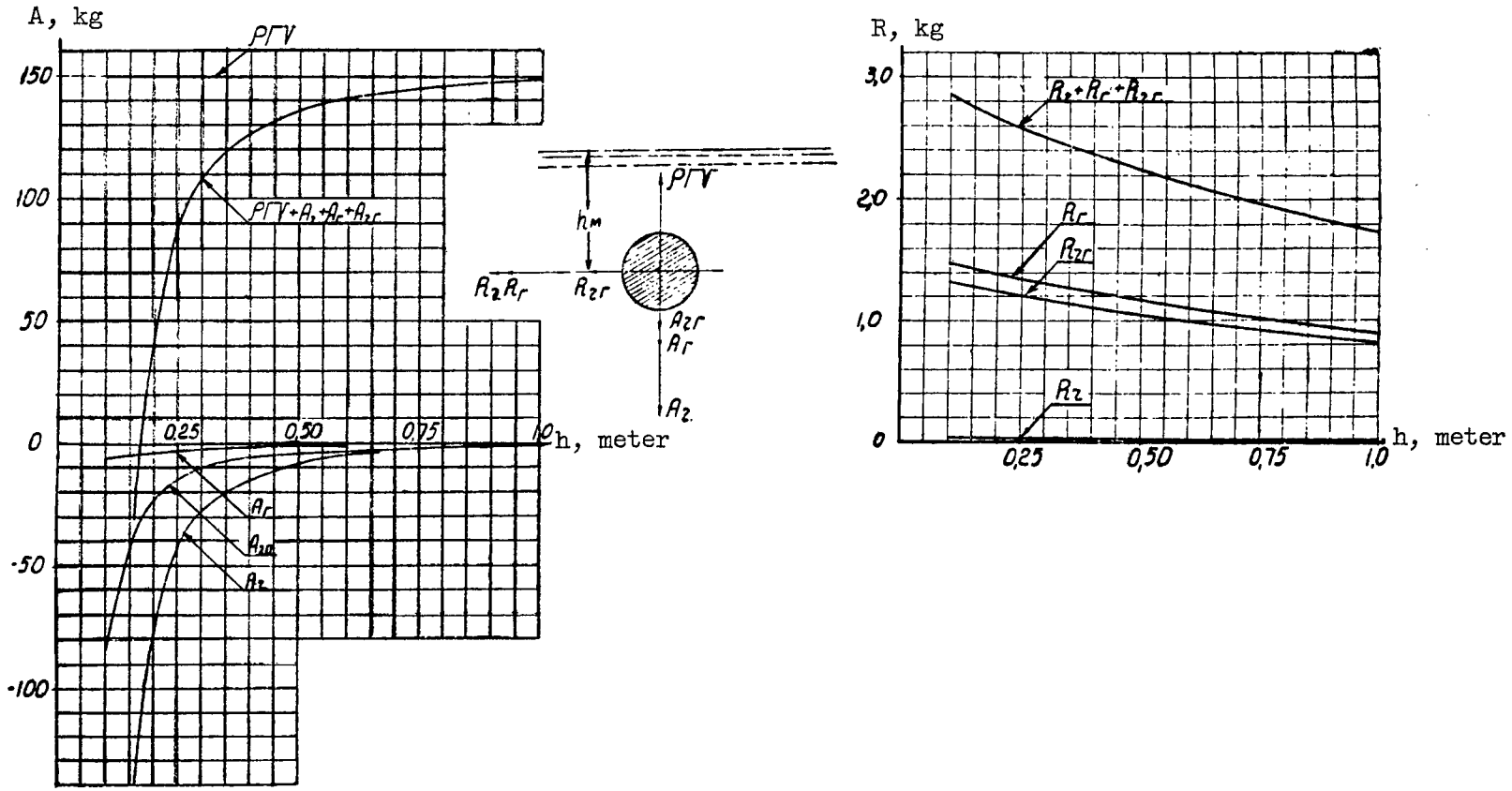

Figure 6. - Dependence of lift and wave resistence of a cylinder with positive circulation on depth of submersion.

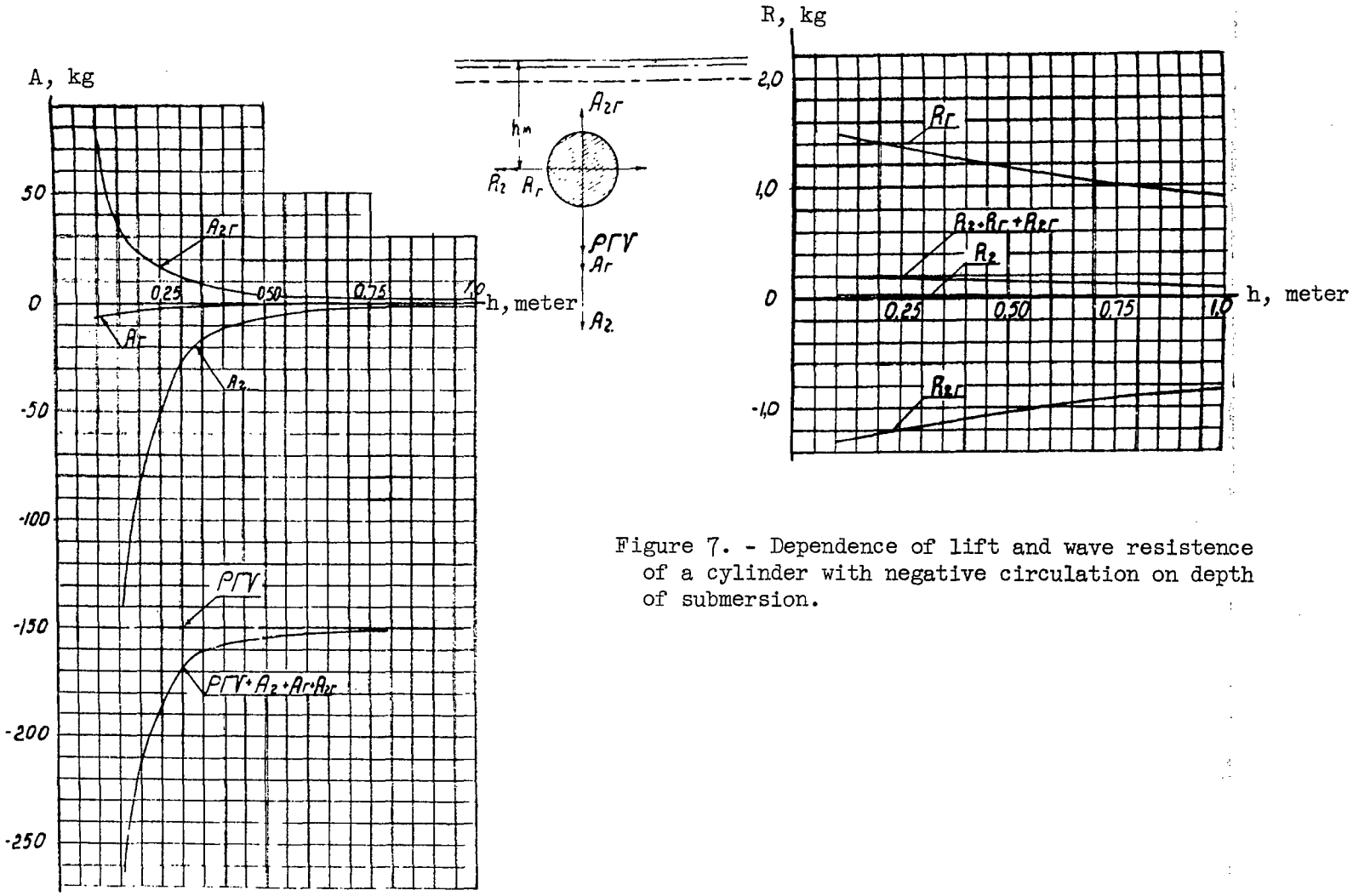

Figure 7. - Dependence of lift and wave resistence of a cylinder with negative circulation on depth of submersion.

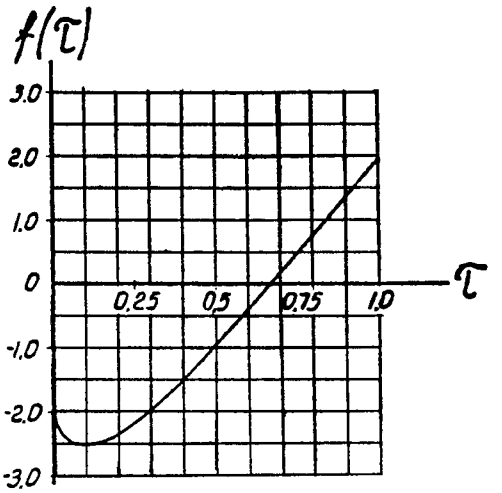

Figure 8. - Effect of $\tau = 2gh/V^2$ on $f(\tau)$ from formula (28a).

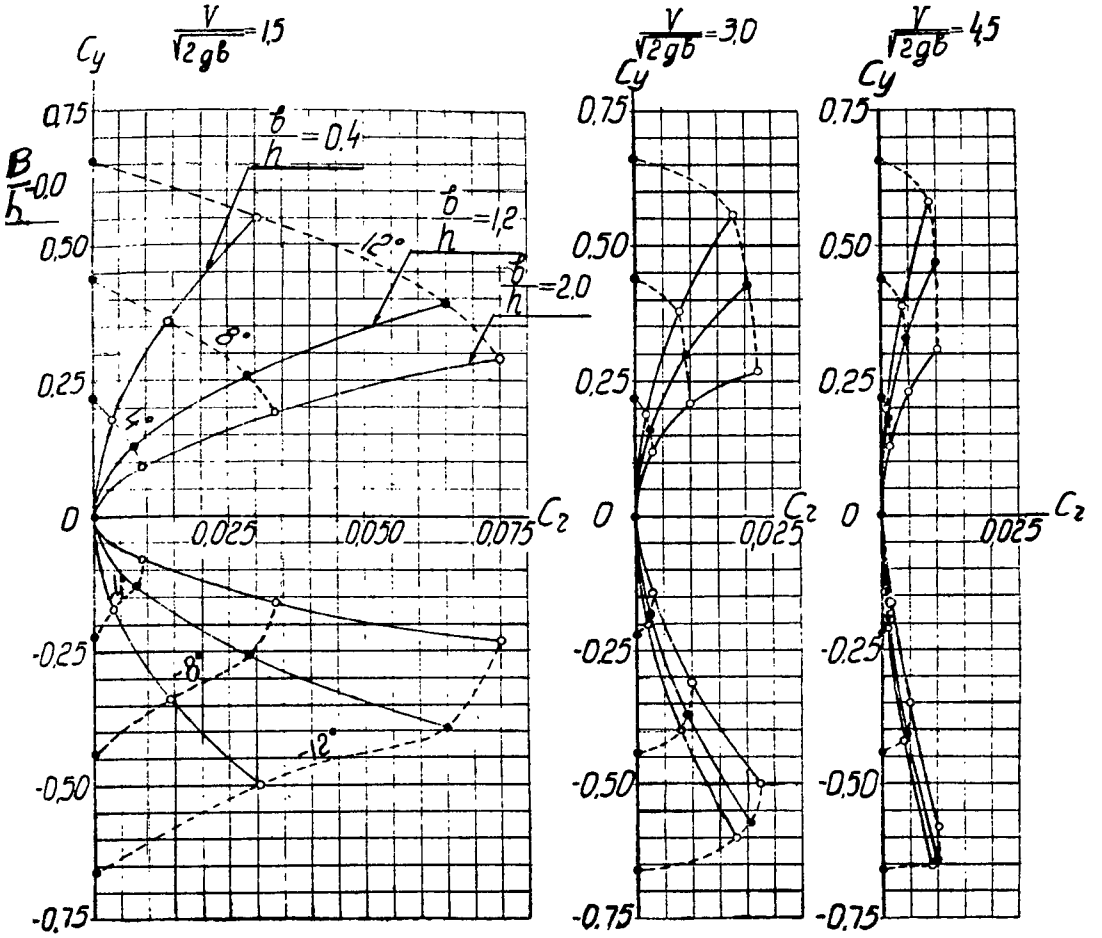

Figure 9. - Polars of foil of infinite span moving in ideal fluid.

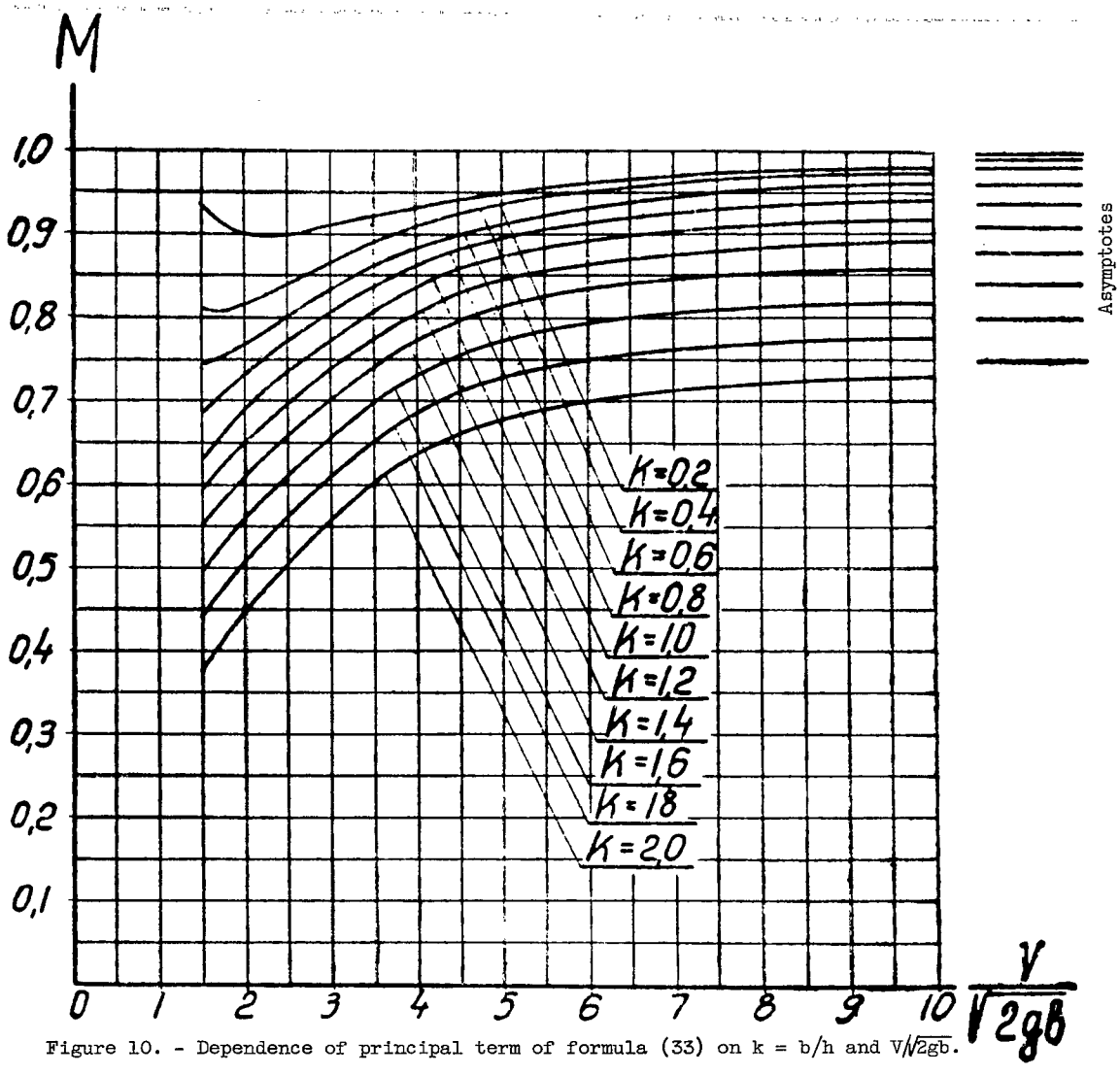

Figure 10. - Dependence of principal term of formula (33) on k = b/h and $V/\sqrt{2gb}$.

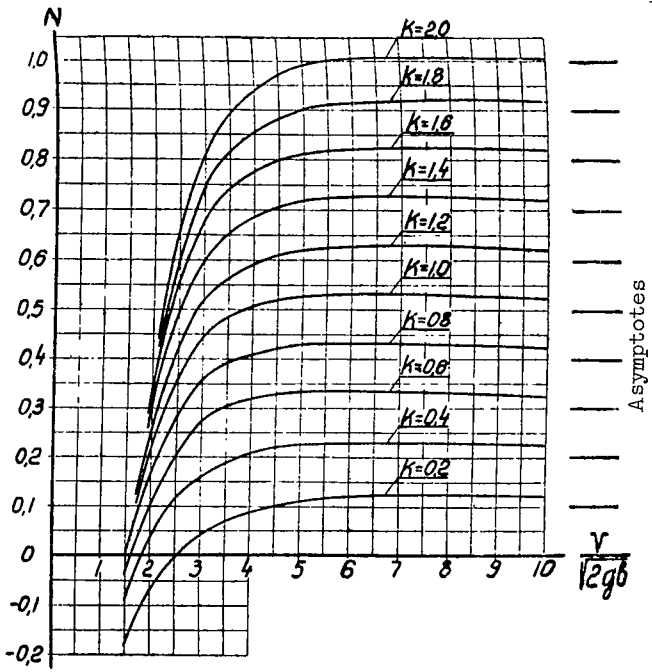

Figure 11. - Dependence of additional term of formula (33) on k = b/h and $V/\sqrt{2gb}$.

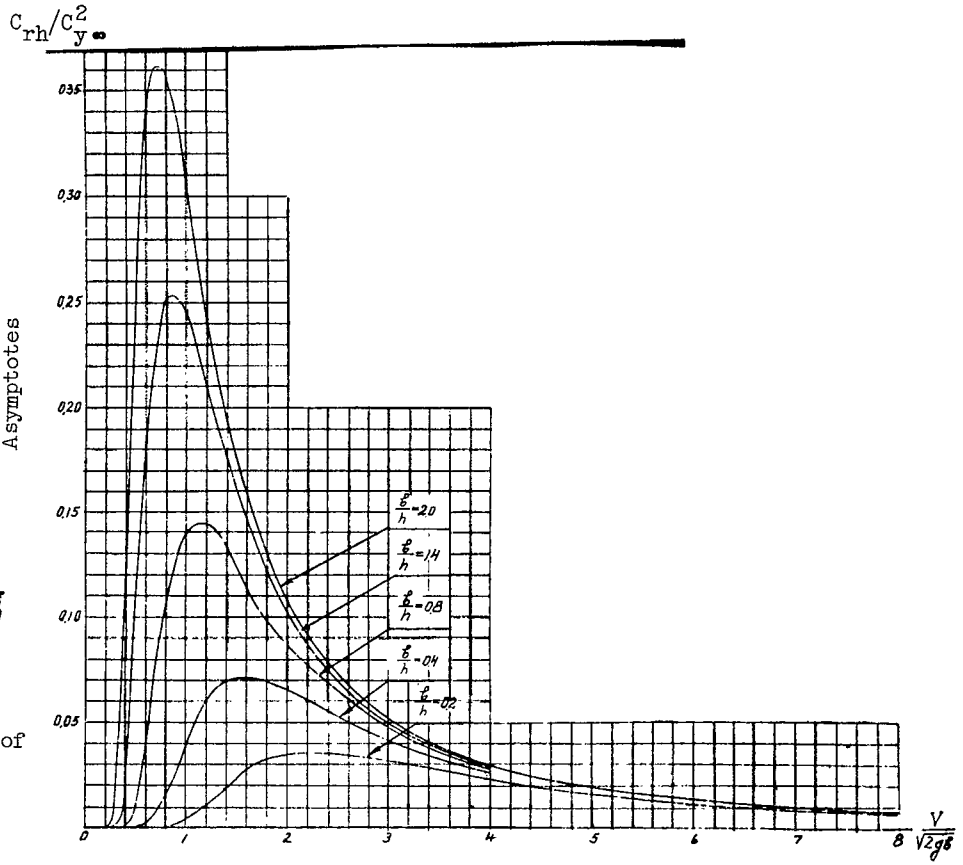

Figure 12. - Dependence of $C_{rh}/C_{y\infty}^2$ from formula (34) on k = b/h and $V/\sqrt{2gb}$.

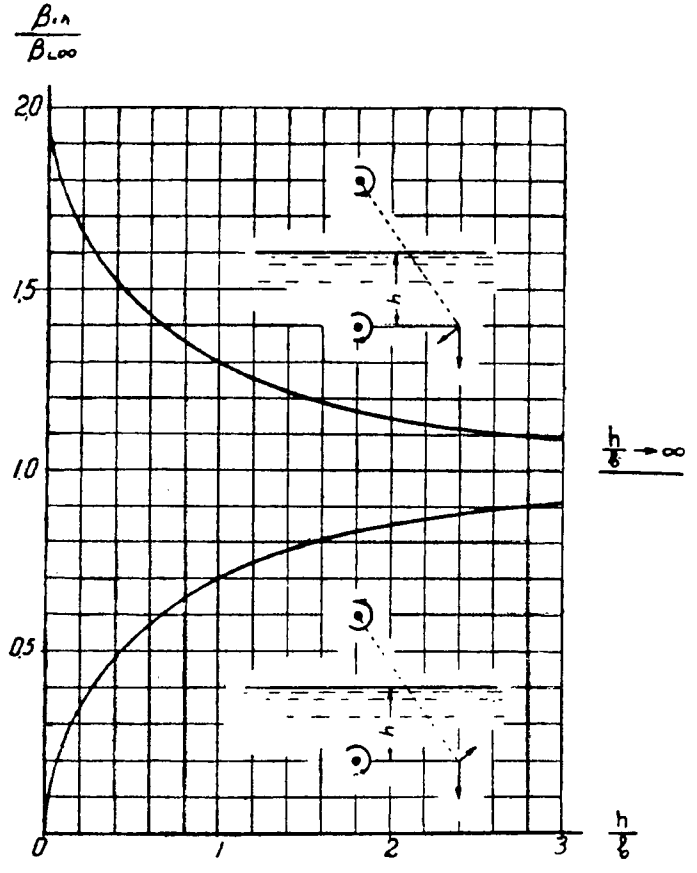

Figure 13. - Dependence of $\beta_{ih}/\beta_{i\infty}$ from formulas (45) and (46) on h/b for the two variants to account for the finite span.

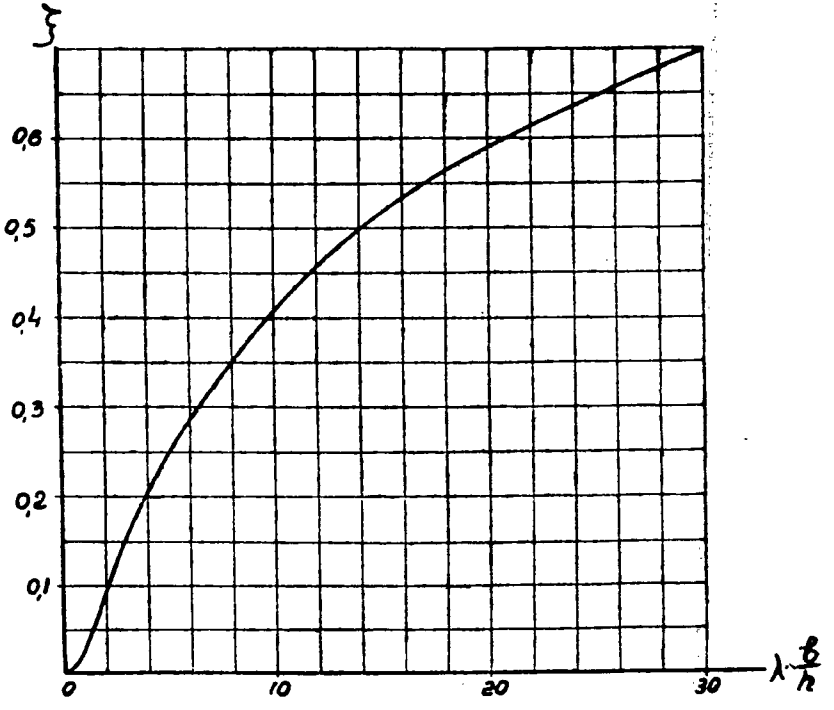

Figure 14. - Effect of $\lambda b/h = l/h$ on the correction ξ from formula (46b).

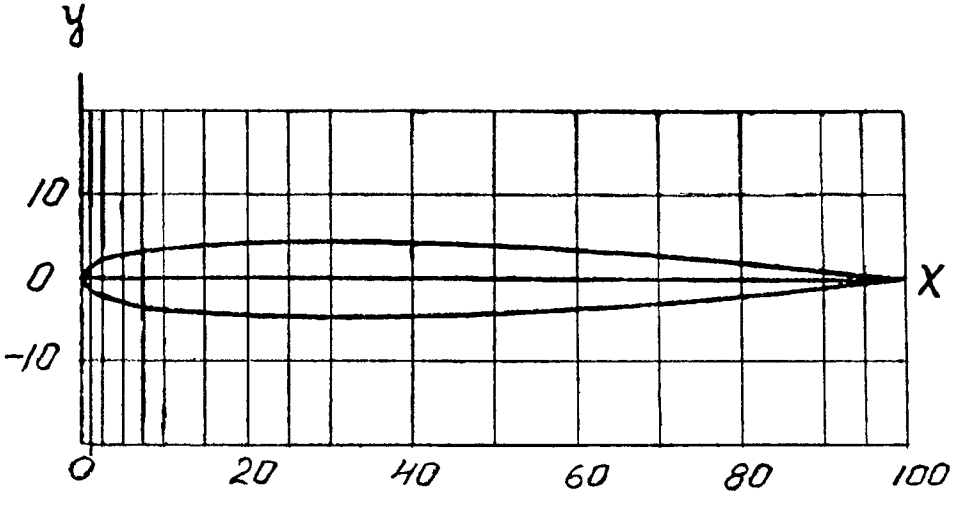

Figure 15. - Coordinates of symmetrical profile NACA 0.0009.

x	y	x	y
0.00	0.00	40.0	± 4.352
1.25	± 1.420	50.0	± 3.971
2.50	± 1.961	60.0	± 3.423
5.00	± 2.666	70.0	± 2.748
7.50	± 3.150	80.0	± 1.967
10.0	± 3.512	90.0	± 1.086
15.0	± 4.009	95.0	± 0.605
20.0	± 4.303	100	± 0.095
25.0	± 4.456	100	0.000
30.0	± 4.501		

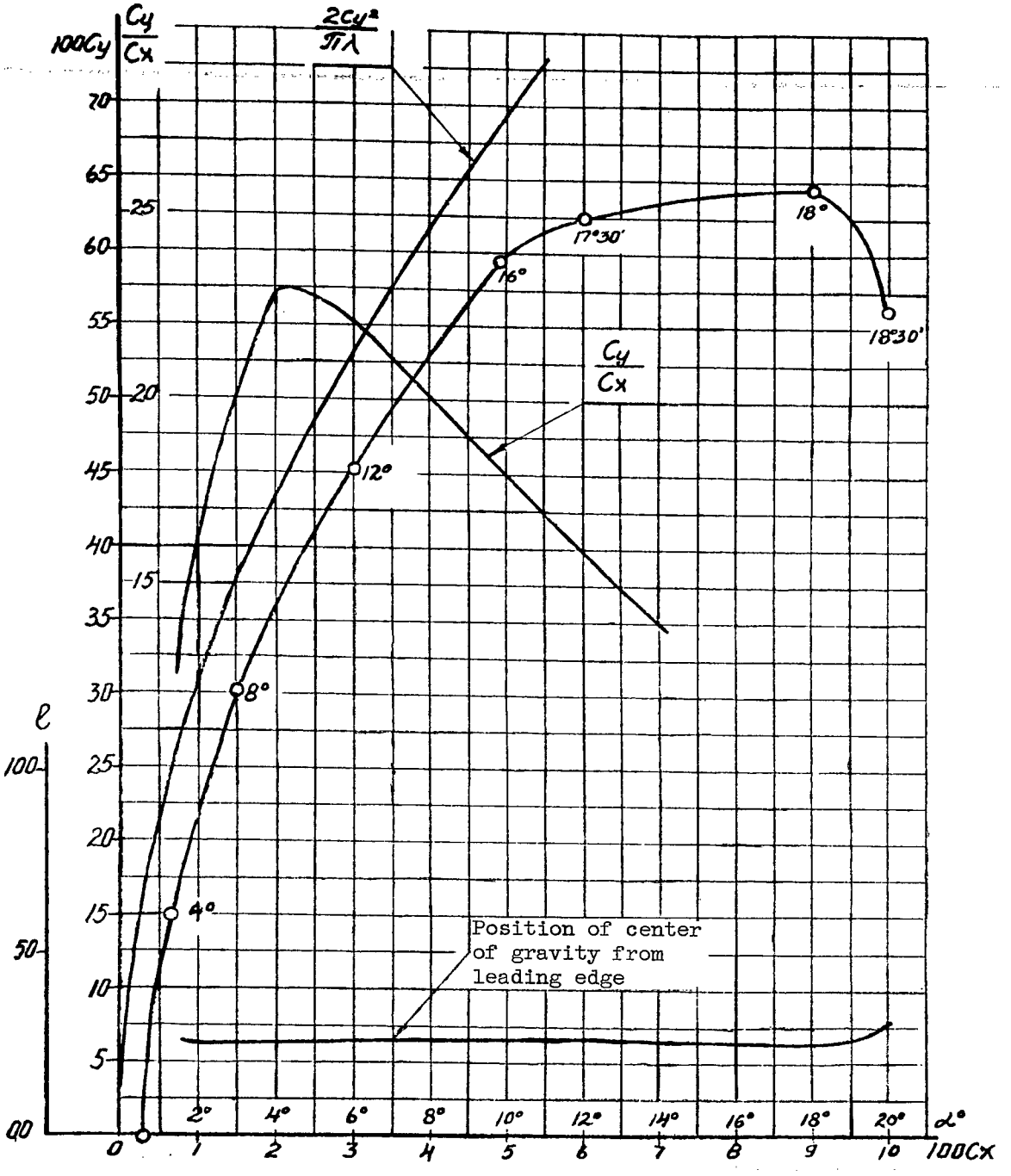

Figure 16. - Aerodynamic characteristics of profile NACA 0.0009.

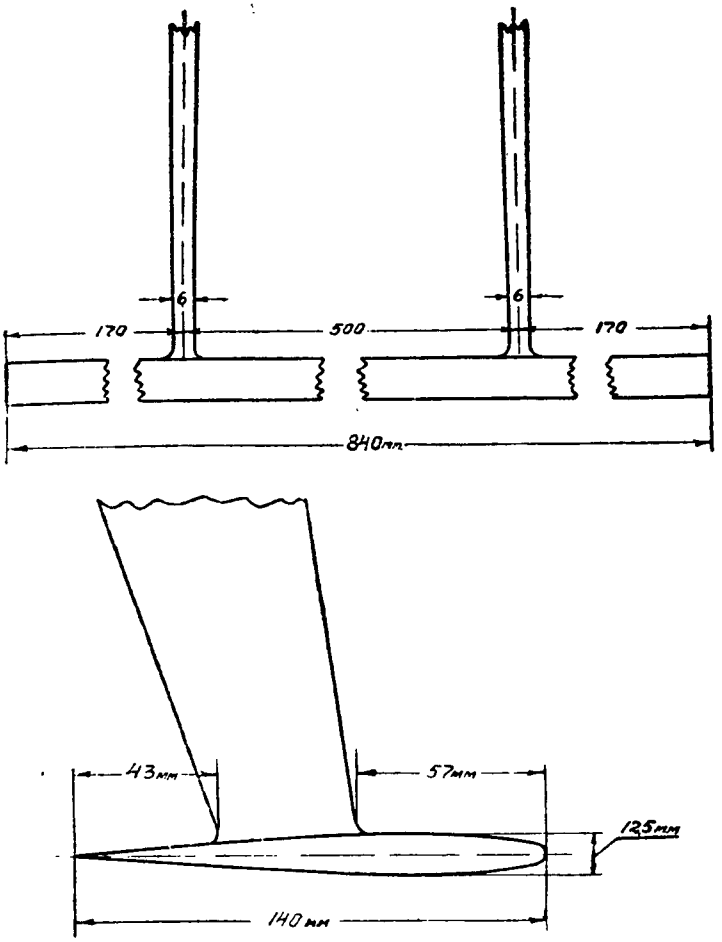

Figure 17. - Scheme of arrangement of supporting brackets on hydrofoil.

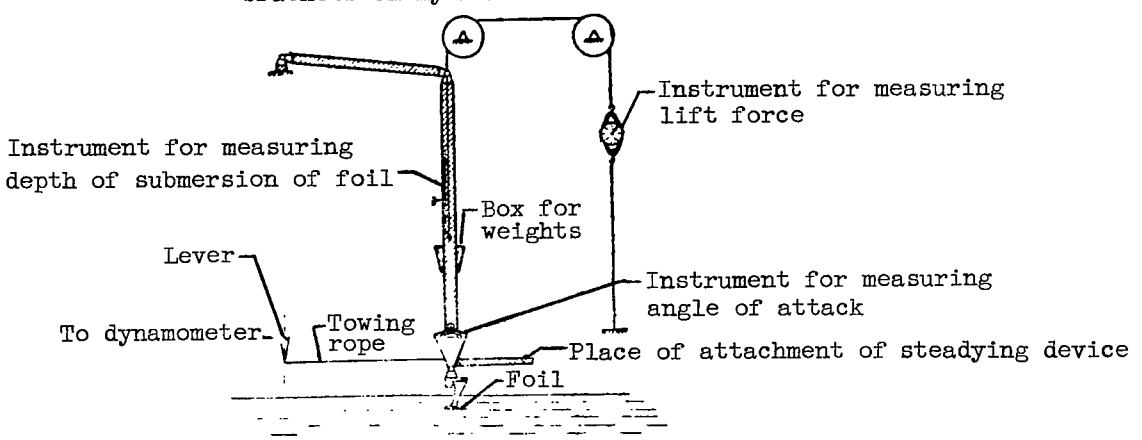

Figure 18. - Set-up for testing the hydrofoil in tank.

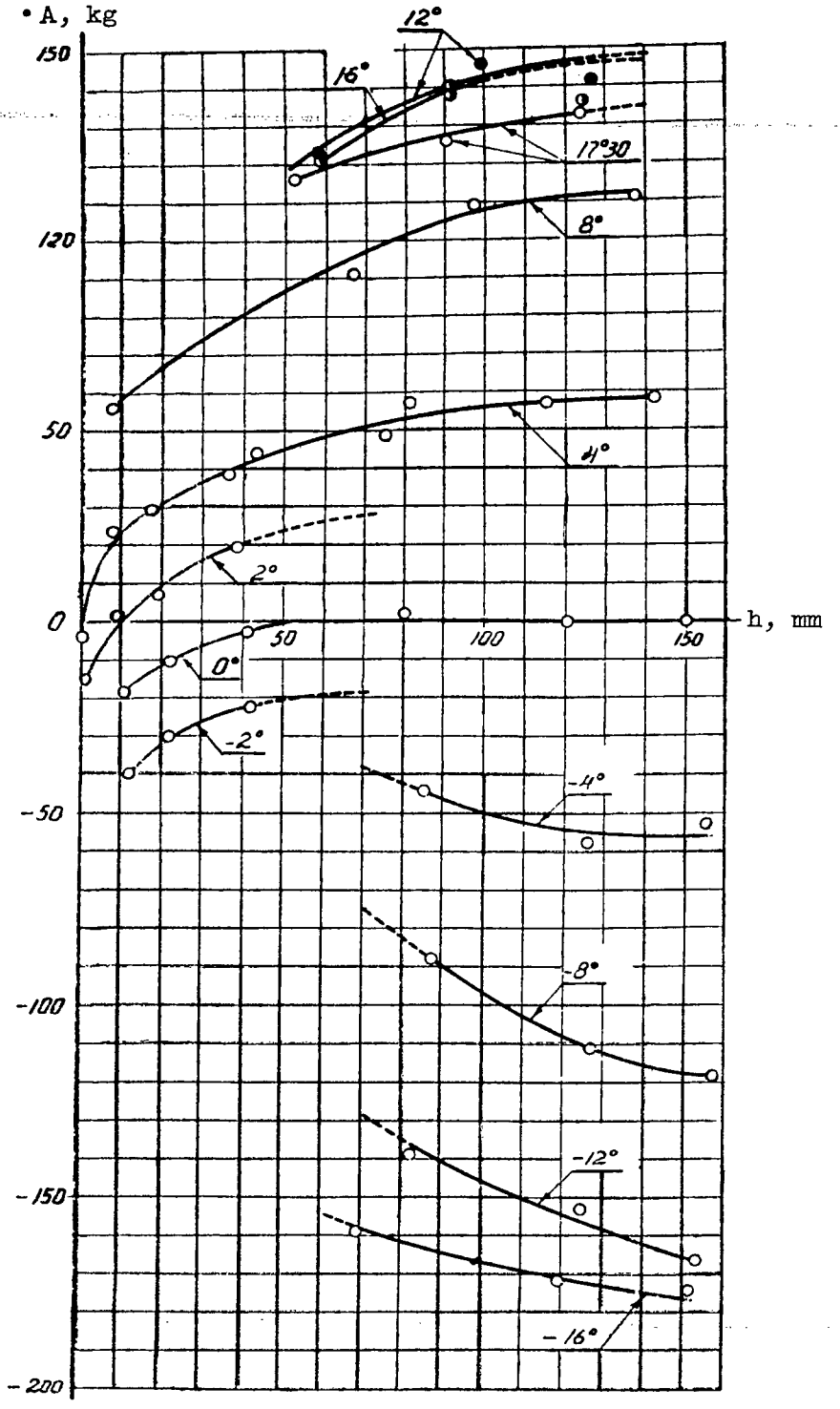

Figure 19. - Dependence of lift of foil on depth of submersion and angle of attach for V = 6 meters per second (test data).

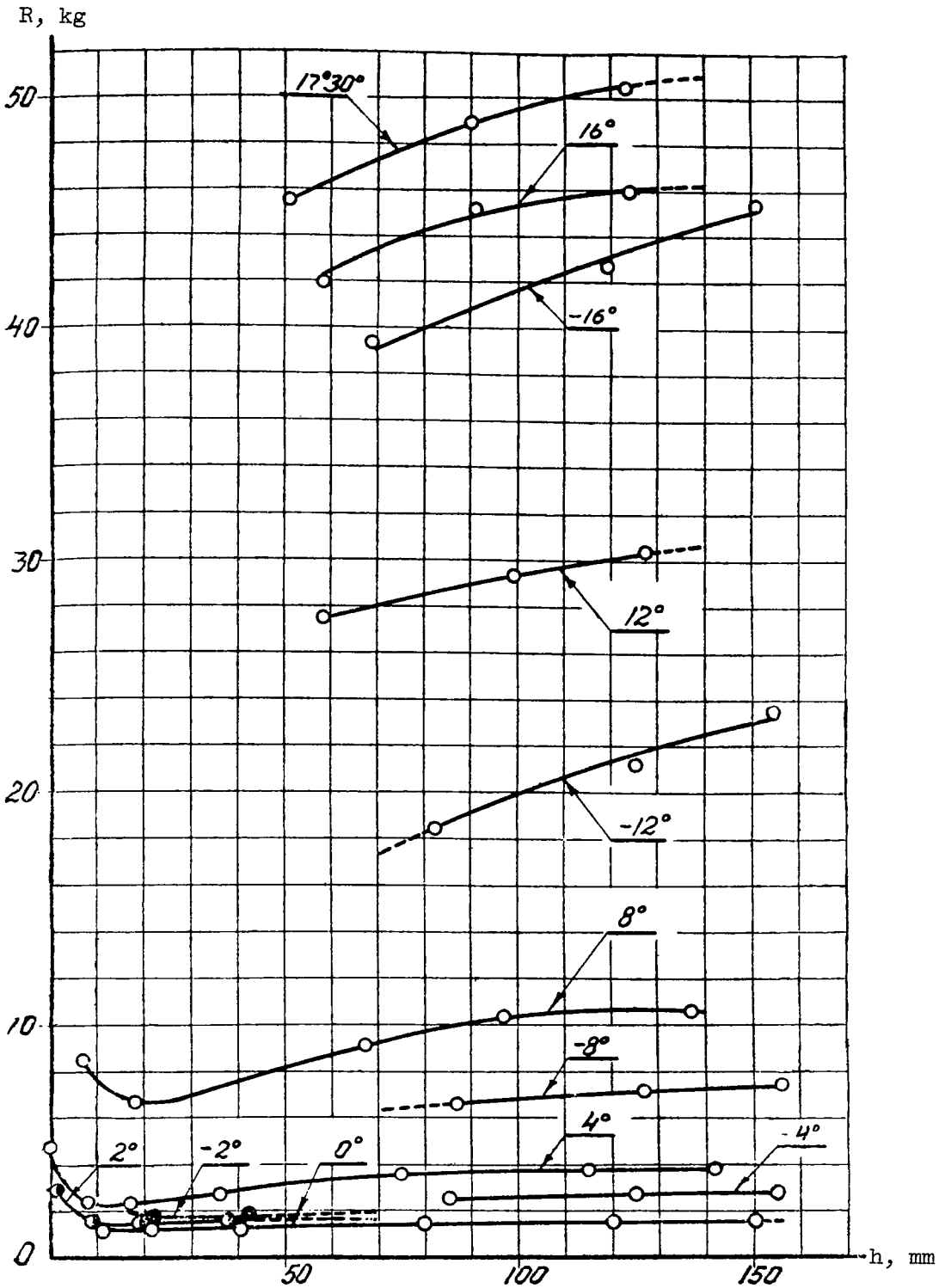

Figure 20. - Dependence of total frontal drag of hydrofoil on depth of submersion and angle of attack for V = 6 meters per second (test data).

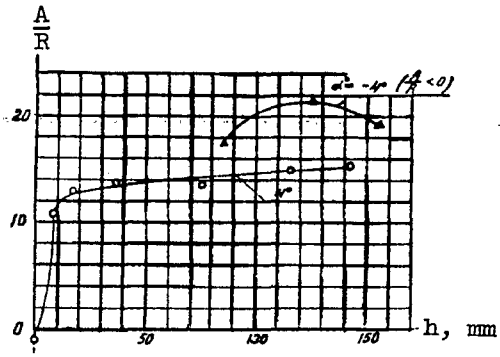

Figure 21. - Dependence of hydrodynamic efficiency of the hydrofoil on depth of submersion for $\alpha = \pm 4^{\circ}$ and V = 6 meters per second. (test data).

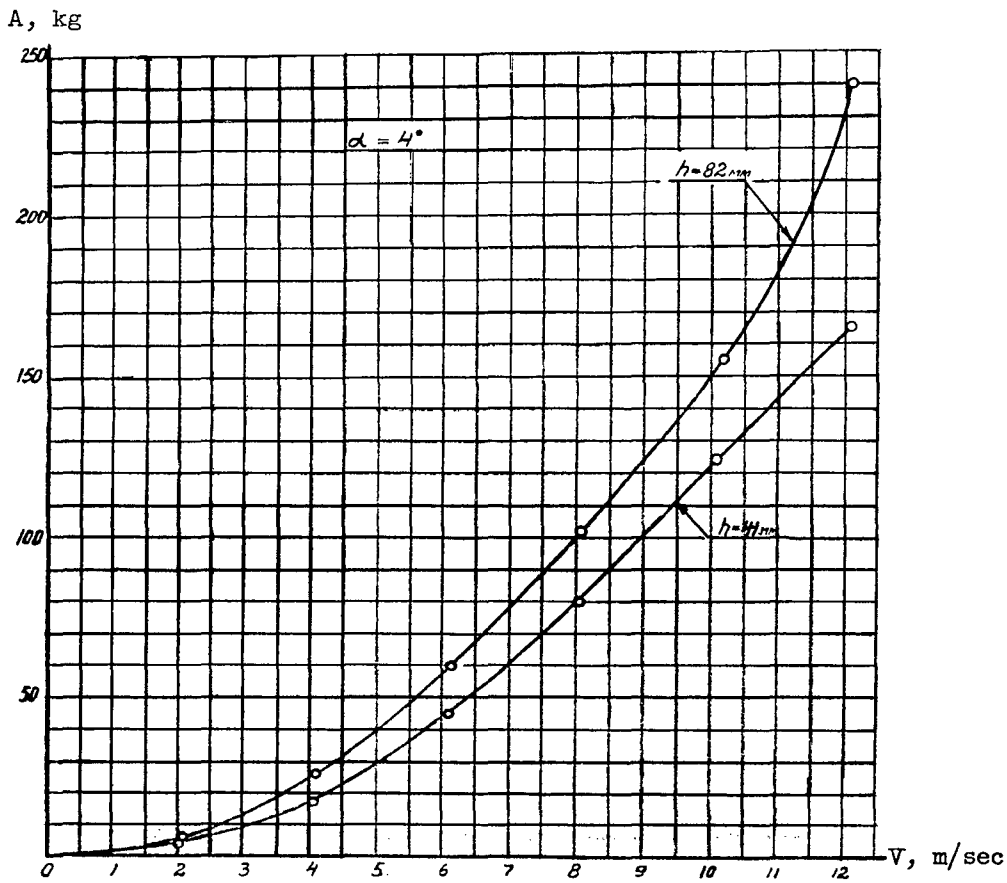

Figure 22. - Dependence of lift of hydrofoil on velocity for $\alpha = 4^{\circ}$ and for two depths of submersion (test data).

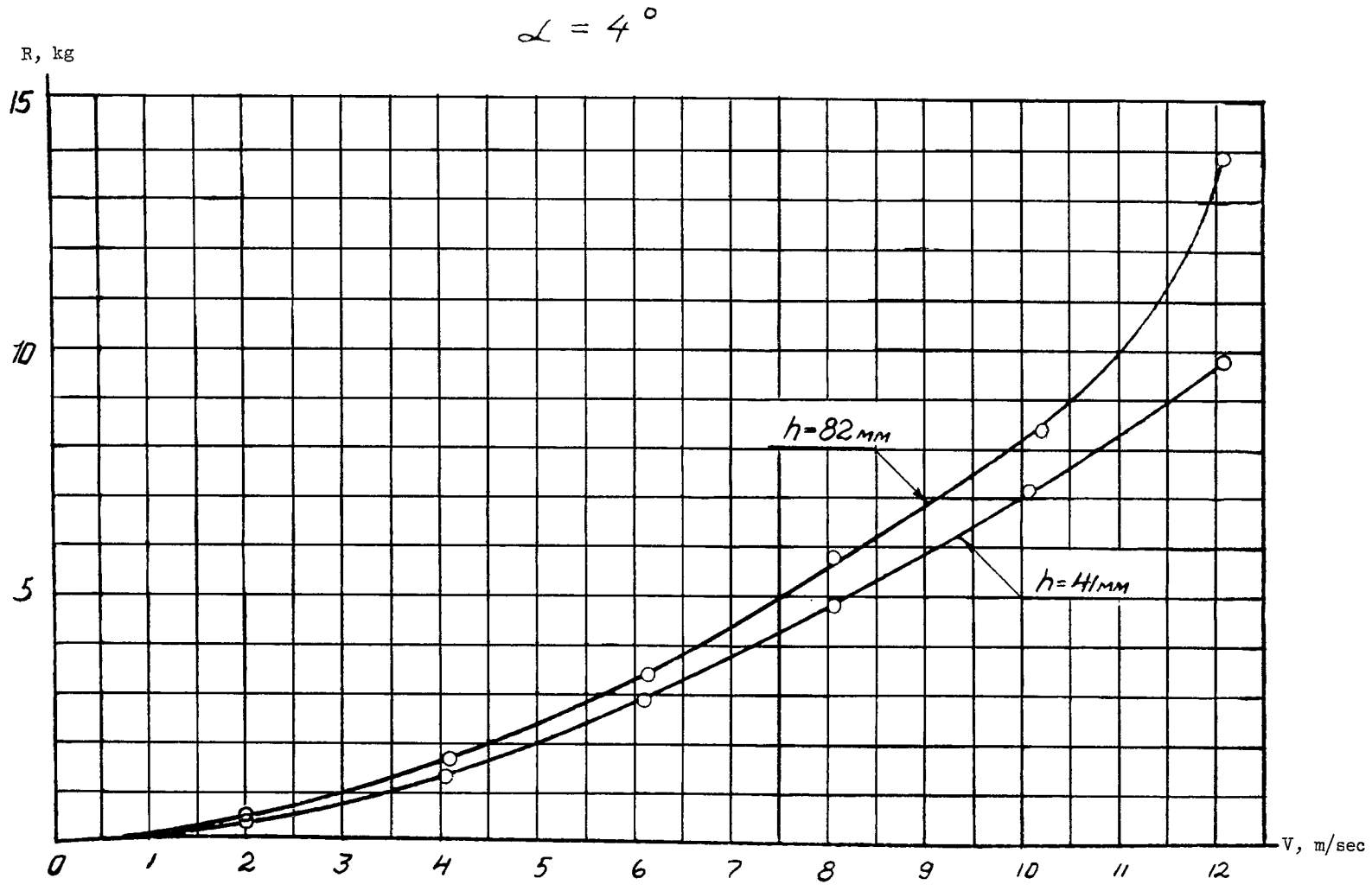

Figure 23. - Dependence of total frontal drag of hydrofoil on velocity for $\alpha = 4^{\circ}$ and for two depths of submersion (test data).

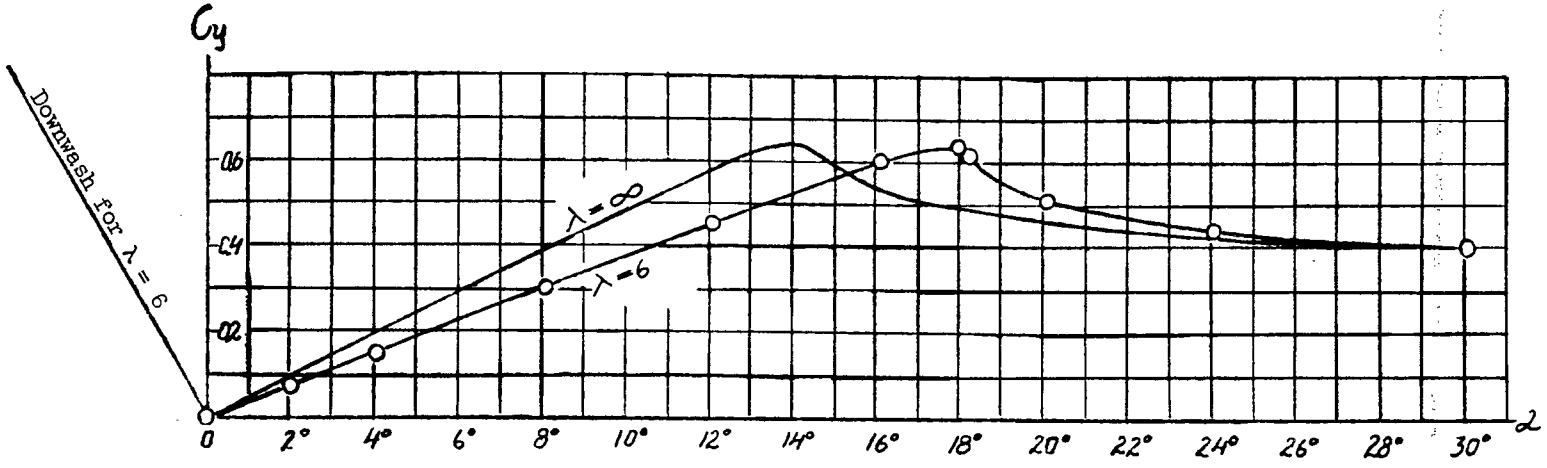

Figure 24. - Aerodynamic lift coefficients of foil of finite and infinite span, respectively.

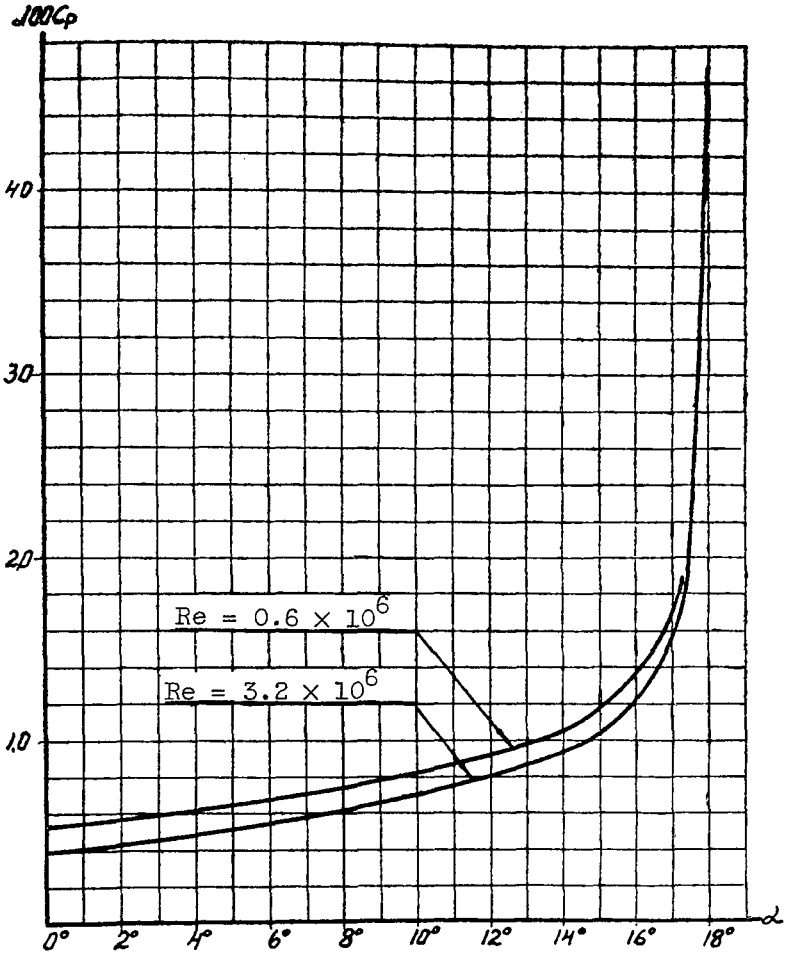

Figure 25. - Dependence of profile drag coefficient on angle of attack and Reynolds number.

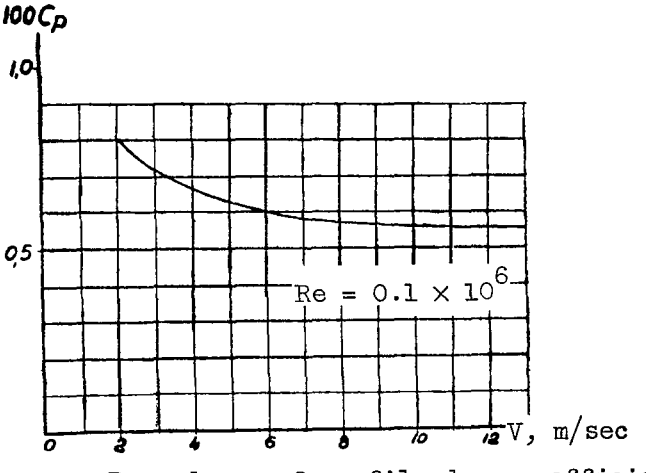

Figure 26. - Dependence of profile drag coefficient on velocity for $\alpha = 4^{\circ}$.

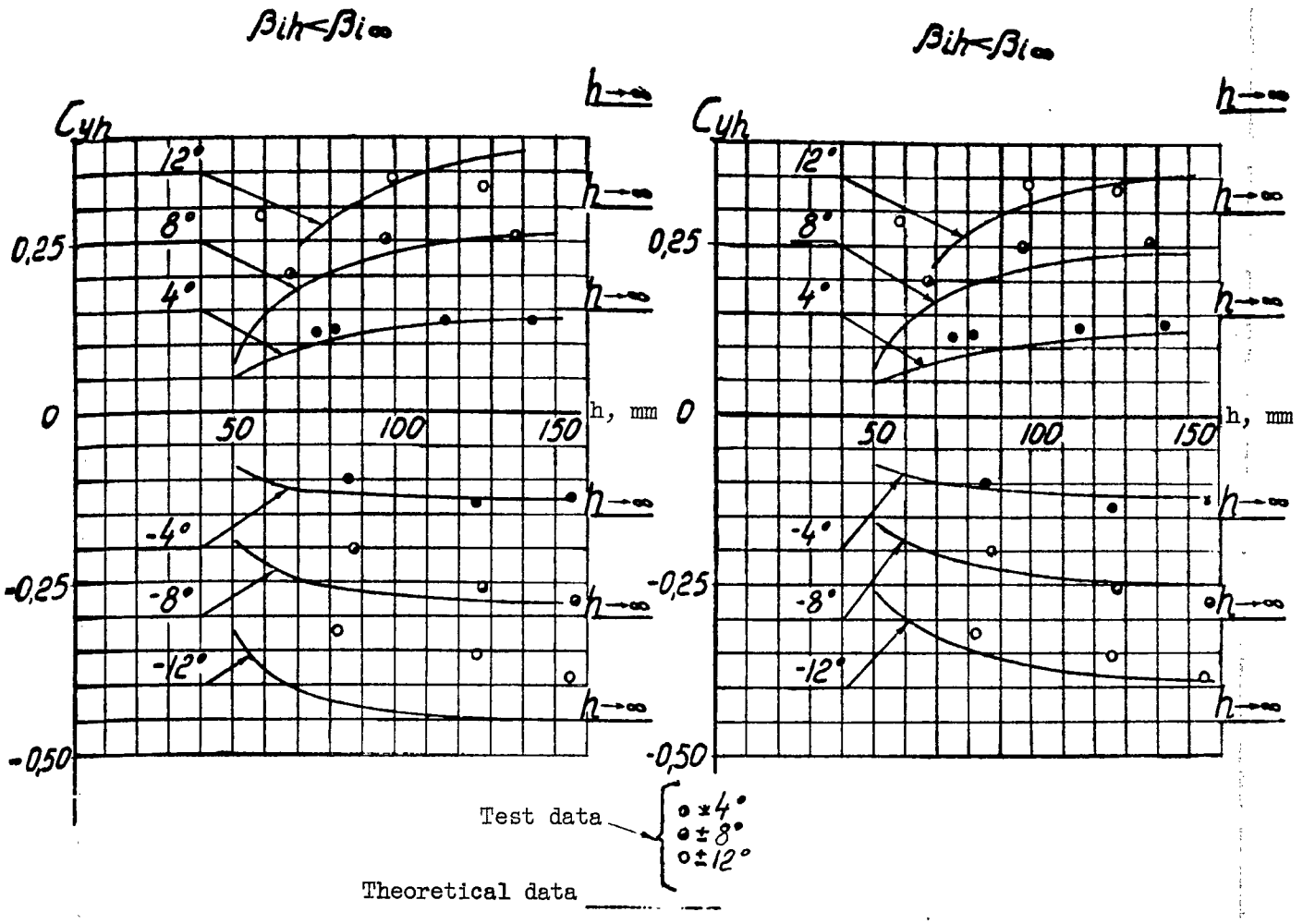

Figure 27. - Comparison of experimental with theoretical results for lift coefficients of hydrofoil for two variants taking into account the finite·span.

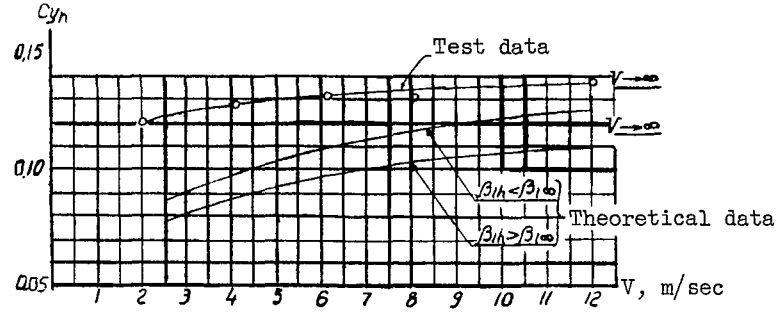

Figure 28. - Comparison of experimental with theoretical results for lift coefficients of a hydrofoil for $\alpha = 4^{o}$ and h = 82 millimeters.

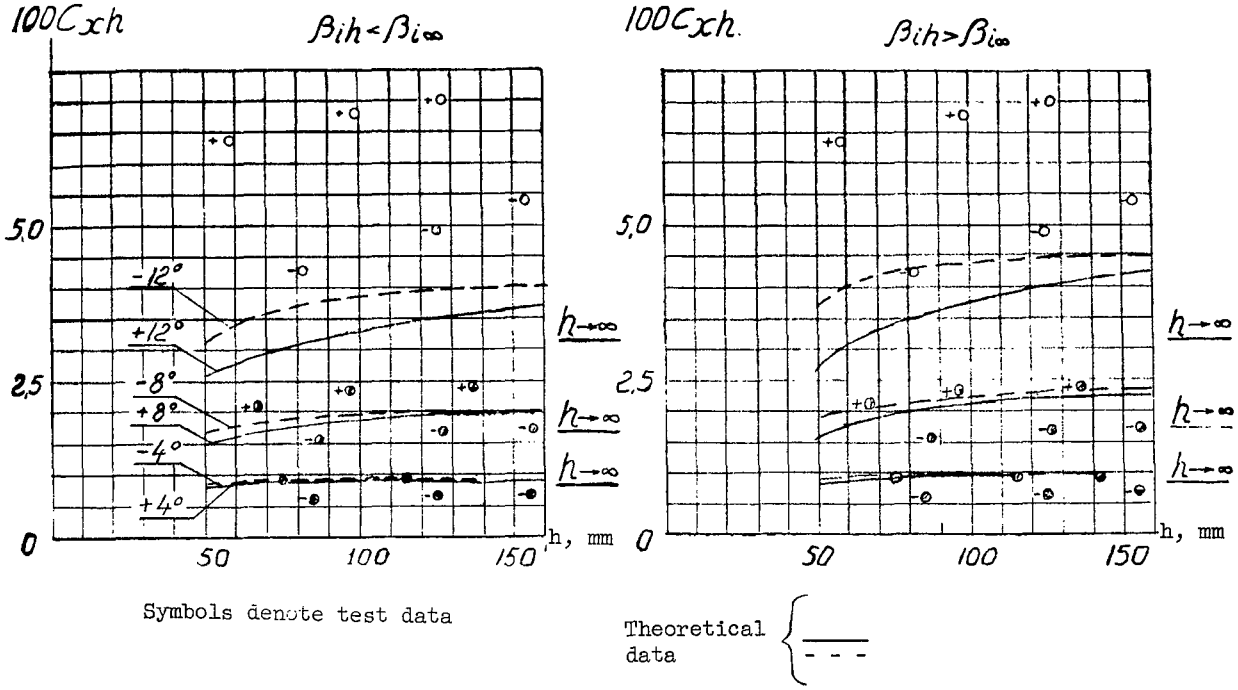

Figure 29. - Comparison of experimental and theoretical coefficients of total drag of a hydrofoil for V = 6 meters per second.

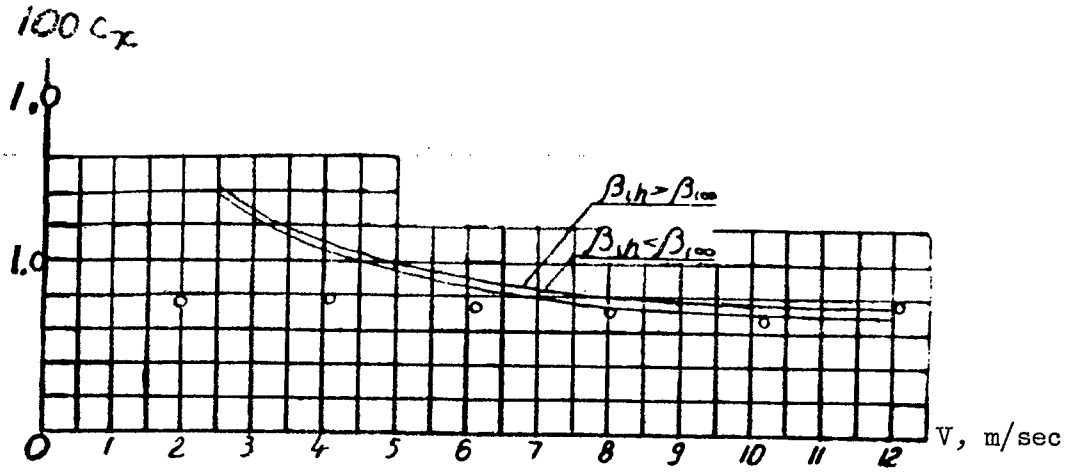

Figure 30. - Comparison of experimental and theoretical coefficients of total drag of a hydrofoil for $\alpha = 4^{\circ}$ and V = 6 meters per second.

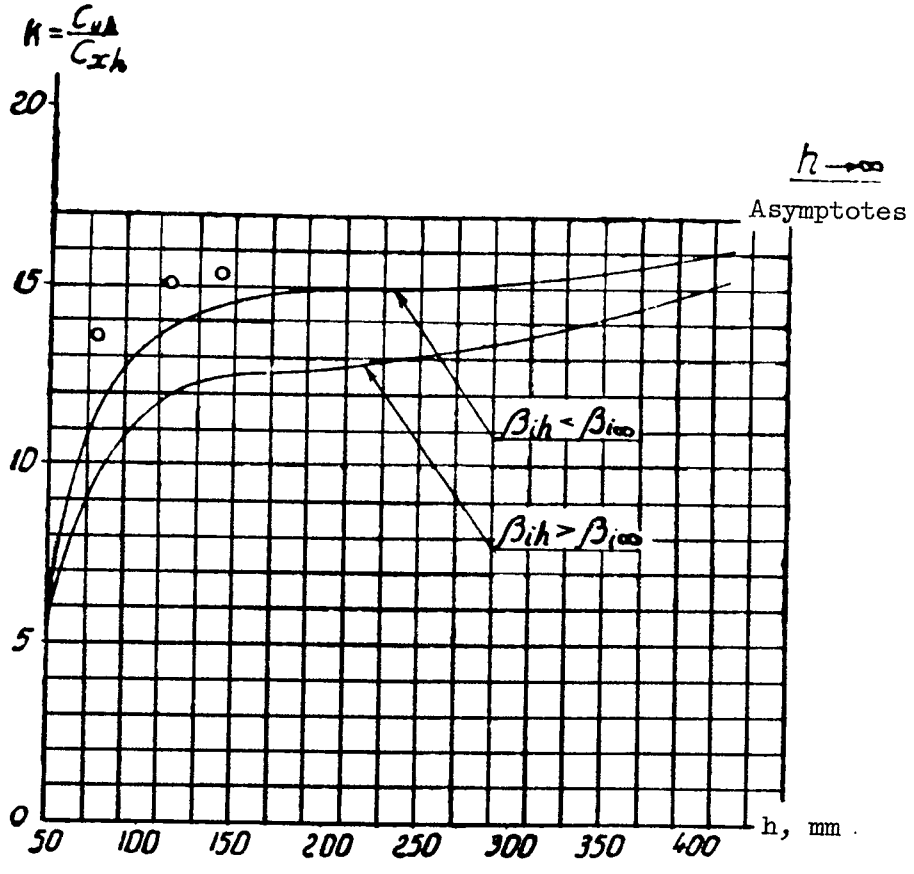

Figure 31. - Comparison of experimental and theoretical hydrodynamic efficiencies of a hydrofoil for $\alpha = 4^{\circ}$ and V = 6 meters per second.

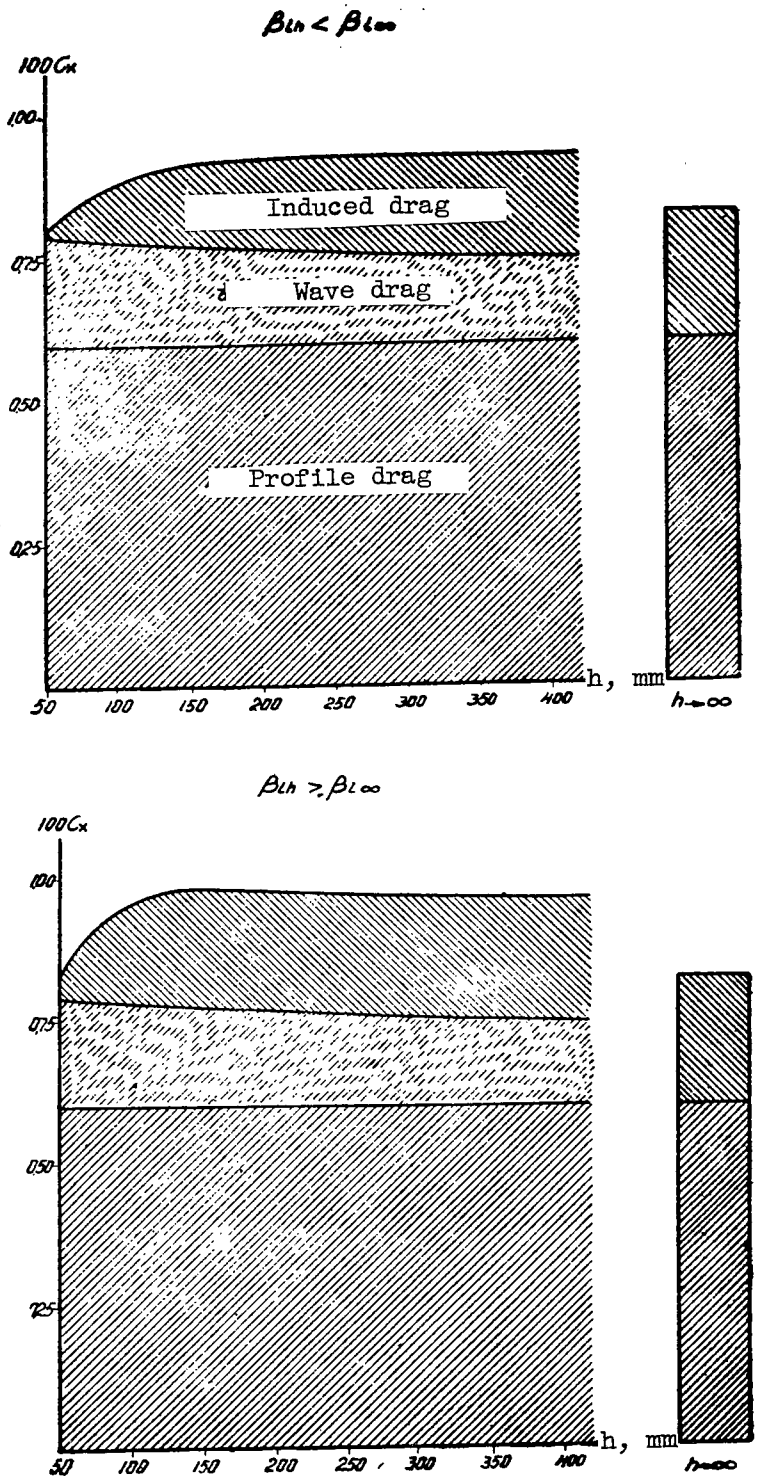

Figure 32. - Effect of depth of submersion of a hydrofoil on the components of its frontal drag for $\alpha = 4^{\circ}$, and V = 6 meters per second, and $\lambda = 6$ (theoretical data).